Res. Lett. Inf. Math. Sci., 2003, Vol.**5**, pp 85-118
Available online at http://iims.massey.ac.nz/research/letters/

Source release rate estimation of atmospheric pollution from a non-steady point source – Part 2: Source at an unknown location

P. Kathirgamanathan[1] , R. McKibbin[2] & R.I. McLachlan[1]

[1] *Institute of Fundamental Sciences*
Massey University, Palmerston North, New Zealand.

[2] *Institute of Information & Mathematical Sciences*
Massey University at Albany, Auckland, New Zealand.

This paper presents an inverse modelling procedure to estimate the location and release rate of atmospheric pollution. The input to this model requires measured pollution concentration at a minimum of three observation sites on the ground and meteorological conditions such as wind speed and cloud cover. The inverse model is formulated as a least squares minimisation problem coupled with the solution of an advection-diffusion equation for a non-steady point source model. Since the minimisation problem has a combination of linear and non-linear parameters the problem is solved in two steps. Non-linear parameters are found by constructing an iterative procedure using an optimisation routine such as *MATLAB*'s *lsqnonlin* and at each iteration, the linear subproblem is solved to estimate the linear parameters. Finding the linear parameters is an ill-posed problem and consequently its solution is extremely sensitive to errors in the data. Tikhonov regularisation, which stabilises the process of the solution, is used to overcome the ill posedness of the problem and the regularisation parameter is estimated using the properties of the non-linear L-curve, linear L-curve and generalised cross validation. Finally, the accuracy of the model is examined by imposing normally-distributed relative noise into concentration data generated by the forward model.

1 Introduction

In our previous papers (11), (12), we categorise the analysis process for accidental gas releases into 4 cases as follows: (1) instantaneous release from a known location, (2) instantaneous release from an unknown location, (3) extended release over a period of time from a known location, (4) extended release over a period of time from an unknown location. In this paper we propose a methodology for Case 4 where pollution originates from a point source with an extended release over a period of time from an unknown location. That is, we consider the problem where the transport properties of the medium are assumed to be known but the location and release history of the pollution must be inferred.

The methodology for estimating the location and release rates of pollution sources is based on the solution of an advection-diffusion equation and a least squares technique. The least squares technique optimises the agreement between measured and model-predicted concentration by varying the model input parameters within reasonable ranges of uncertainties. In the solution process, the unknown release rate function is discretised into many components. The relationship between the concentration of pollution, C, and the discretised components is linear and that between C

and the location parameters is non-linear. Therefore the problem involves estimating both non-linear and linear parameters. In one of our previous papers (12) it has been shown that estimating linear parameters (release rates) for given non-linear parameters (location) is a linear ill-posed problem. Therefore estimating release rates from a source of unknown location is a non-linear ill-posed problem. This problem is further complicated by inexact information. In reality, the data contains measurement errors, so the true solution will not fit the data. Also the meteorological parameters are not known exactly. In this model, these values are assumed to be uniform and constant; however in reality, they do vary in space and time and are difficult to model accurately.

We shall use Tikhonov's regularisation to overcome the ill-posedness of the problem. In this method, the sum of two components is minimised: a norm of data misfit and a norm of linear model parameters. Balancing the two components is controlled by a regularisation parameter. We solve the problem by constructing an iterative procedure for the nonlinear parameters, where at each iteration a linear problem is solved. We have slightly modified the L-curve criterion developed by Hansen (8) for linear ill-posed inverse problems to our nonlinear problem. We use this criterion as well as Wahhba's (2) 'leaving-out-one' lemma to estimate the optimal value of the regularisation parameter for this problem.

2 The Inverse Model

A Cartesian co-ordinate system (X, Y, Z) is used with the X-axis oriented in the direction of the mean wind, the Y-axis in the horizontal cross-wind direction, and the Z-axis oriented in the vertical direction as in Figure 28. In the estimation of the source term parameter problem, the location and release rate of the pollutant at source are not available, but the concentration of pollutant distribution at some down-stream locations such as $P = (X_0, Y_0, 0)$, $Q = (X_0 + x_1, Y_0 + y_1, 0)$, and $R = (X_0 + x_2, Y_0 + y_2, 0)$ are available, where X_0, Y_0 are unknown and x_1, x_2, y_1 and y_2 are known. Our goal here is to estimate the release rate $q(t)$ of the pollution and its location such as X_0, Y_0 and H. Here, H is a height of the source of a pollution from the ground.

We use the concentration measurements at the down-stream location P, Q, R along with the equation

$$\begin{aligned} C &= \int_0^t \frac{q(\tau)}{8\pi^{\frac{3}{2}} (K_x K_y K_z)^{\frac{1}{2}} (t-\tau)^{\frac{3}{2}}} \times \exp\left[-\frac{(X - U(t-\tau))^2}{4K_x(t-\tau)} - \frac{Y^2}{4K_y(t-\tau)} \right] \\ &\quad \times \left(\exp\left[-\frac{(Z-H)^2}{4K_z(t-\tau)} \right] + \exp\left[-\frac{(Z+H)^2}{4K_z(t-\tau)} \right] \right) d\tau \end{aligned} \tag{2.36}$$

to estimate the source release rate and its location. This is an inverse problem. Source release rate estimation is an ill-posed problem. Even if the measured data are error free, the solution to the release rate estimation problem is not stable. In order to stabilise the solution, regularisation methods must be used. Measured concentration data usually contain measurement errors. As a result, $q(t)$, X_0, Y_0 and H recovered by this inverse analysis are not exact and are only estimates within the measurement and regularisation errors.

The concentration of pollutant at a point $(X_0, Y_0, 0)$ can be expressed as

$$C(X_0, Y_0, 0, t) = \int_0^t K(t, \tau) q(\tau) d\tau, \tag{2.37}$$

where the kernel $K(t, \tau)$ is

$$K(t,\tau) = \frac{\exp\left[-\frac{(X_0 - U(t-\tau))^2}{4K_x(t-\tau)} - \frac{Y_0^2}{4K_y(t-\tau)} - \frac{H^2}{4K_z(t-\tau)} \right]}{4\pi^{\frac{3}{2}} (K_x K_y K_z)^{\frac{1}{2}} (t-\tau)^{\frac{3}{2}}}. \tag{2.38}$$

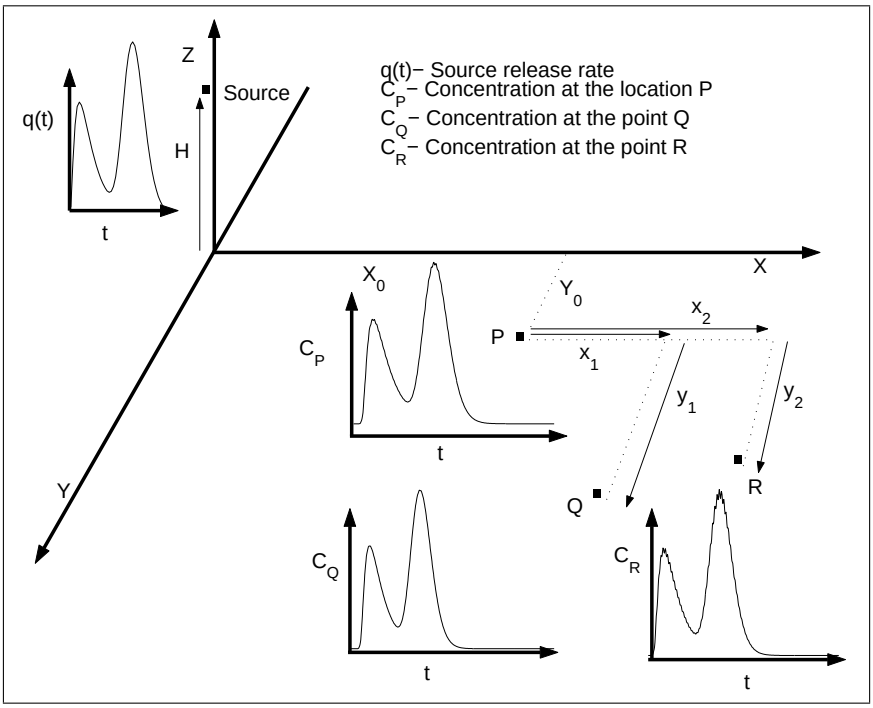

Figure 28: Illustration of the inverse problem

2.1 The least-squares formulation

It is assumed that $n+1$ concentration values $C_i = C(X_0, Y_0, 0, t_i)$ are measured at the point $(X_0, Y_0, 0)$ at equal time intervals between $t_0 = \tau_0$ and $t_n = \tau_m$. The simplest way to proceed is to solve (2.37) on a mesh with uniform spacing. We suppose that we wish to determine the source release at times $\tau_0 = 0, \ldots, \tau_m = t_n$, where $m < n$ since the number of parameters to be estimated should be no greater than the number of data points. Discretising (2.36) by the trapezoidal rule gives the system of equations

$$\mathbf{c} = \mathrm{A}(\mathbf{p})\mathbf{q} \tag{2.39}$$

where $\mathbf{c} = [C(0), \ldots, C(t_n)]^T$, $A_{ij} = K(t_i, \tau_j)\beta_{ij}$, $\mathbf{q} = [q(\tau_0), \ldots, q(\tau_m)]^T$ and $\mathbf{p} = [X_0, Y_0, H]^T$, and where β_{ij} is a quadrature weight. Generally, minimising an objective function solves inverse problems. Now the problem for estimating the release rate $\mathbf{q}$ and the location $\mathbf{p}$ is

$$\text{minimise} \qquad Z(\mathbf{q},\ \mathbf{p}) = \|A(\mathbf{p})\mathbf{q} - \mathbf{c}\|_2^2, \tag{2.40}$$

where $A(\mathbf{p})\mathbf{q}$, $\mathbf{c}$ are vectors containing the estimated and measured concentrations respectively, $\mathbf{p}$ is the vector of unknown non-linear parameters identifying the source location, and $\mathbf{q}$ is the vector of unknown linear parameters identifying the source release rates. The estimated concentrations are obtained from the solution of the forward problem using estimates of unknown parameter values.

Since the minimisation problem given in (2.40) has a combination of linear $\mathbf{q}$ and non-linear parameters $\mathbf{p}$, we separate the solution process into two steps. We find the non-linear parameter $\mathbf{p}$ by constructing an iterative procedure, where at each iteration a linear sub-problem is solved to estimate the linear parameter $\mathbf{q}$ corresponding to that particular value of $\mathbf{p}$. In Chapter 5 we solved the same problem given in (2.40) for a known value of $\mathbf{p}$. It was shown that the problem is ill-posed and we therefore used Tikhonov's regularisation to solve the problem. This means that the linear sub-problem inside the nonlinear iteration is an ill-posed problem.

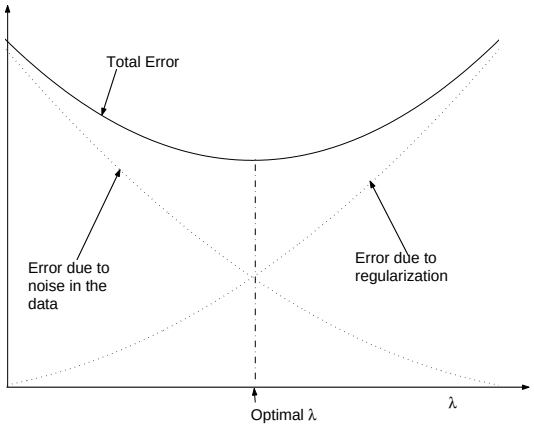

Figure 29: Error in Tikhonov's regularisation method

2.2 Regularized least squares

Tikhonov's regularization replaces the ill-posed problem with the well-posed problem by imposing a bound on the solution. With Tikhonov's regularisation, we introduce the regularised objective function

$$\begin{aligned} Z(\mathbf{q},\ \mathbf{p}) &= \|A(\mathbf{p})\mathbf{q}-\mathbf{c}\|_2^2+\lambda^2\|L\mathbf{q}\|_2^2, \\ &= \phi_d+\lambda^2\phi_m, \end{aligned} \tag{2.41}$$

here, $\phi_d = \|A(\mathbf{p})\mathbf{q}-\mathbf{c}\|_2^2$ is the residual norm (or data misfit function), and $\phi_m = \|L\mathbf{q}\|_2^2$ is the solution norm. We will be interested in the function $Z(\mathbf{q},\mathbf{p})$ and its local and global minima with respect to $(\mathbf{q},\mathbf{p})$ for different values of the regularisation parameter λ. Note that the objective function Z is the 2-norm of the following system of equations

$$\begin{bmatrix} A(\mathbf{p}) \\ \lambda L \end{bmatrix}\mathbf{q} = \begin{bmatrix} \mathbf{c} \\ 0 \end{bmatrix}, \tag{2.42}$$

where L is the regularisation operator and λ is the regularisation parameter that controls the relative strength of L, i.e. it compromises between the accuracy and the stability of the solution. The most common form of regularisation operator is

$$\|L\mathbf{q}\|^2 \approx \int_0^{t_n}\left(\frac{d^N q}{d\tau^N}\right)^2 d\tau. \tag{2.43}$$

The most popular choice for obtaining a smooth solution is $N=2$ (17). We also found in previous chapters that $N=2$ gives the best combination of good fit to the data and the smooth solution. When $N=2$, the second derivative of the solution is minimised and therefore L is given by

$$L = \begin{pmatrix} 1 & -2 & 1 & 0 & 0 & \dots \\ 0 & 1 & -2 & 1 & 0 & \dots \\ 0 & 0 & 1 & -2 & 1 & \dots \\ \vdots & \vdots & \vdots & \vdots & \vdots & \vdots \end{pmatrix} \in \mathbf{R}^{(m-1)\times(m+1)}.$$

The total true error of this method has the form shown in Figure 29. The error due to regularisation approaches zero as $\lambda \to 0$, while the error due to noise in the data increases as $\lambda \to 0$. Selection of the optimal regularisation parameter is based on minimising the total error. In a real

situation, we do not know the true error and therefore the curves in Figure 29 cannot be computed unless we know the exact solution. Therefore we have to find a strategy for the choice of the regularisation parameter. In the following section we explore the use of different techniques to find the regularisation parameter.

3 Selection of the regularization parameter

The non-linear problem (2.41) is different from the linear problem (12) in several ways. First, we can't use only linear algebra to determine the minima of Z. Second, the non-linear objective Z may have more than one minimum for each value of λ. In the course of my research I developed a number of different algorithms, each of which is applied to many test cases. The implementation of all the algorithms has a number of features in common. First, we frequently have to determine local minima of $Z(\mathbf{q}, \mathbf{p})$ for a given λ. In all my algorithms this is done by exploiting the fact that some of the variables, namely $\mathbf{q}$, appear in (2.41) linearly and hence can be determined using simple linear algebra: for given values of $\mathbf{p}$ and λ we define $\mathbf{q}(\mathbf{p}, \lambda)$ as the value which minimizes $Z(\mathbf{q}, \mathbf{p})$. This is computed in directly in $MATLAB$ as the least-squares solution of (2.41). For the computation of the local minimum of $Z(\mathbf{q}, \mathbf{p})$ closest to a given point $(\mathbf{q}, \mathbf{p})$ I then relied exclusively on $MATLAB$'s routine *lsqnonlin*. However, this is speeded up enormously because, after the elimination of $\mathbf{q}$ using linear algebra, only three non-linear variables ($\mathbf{p} = [X_0, Y_0, H]$) remain.

3.1 Method 1- variable λ

As discussed earlier, for computing the non-linear parameter $\mathbf{p}$, we solve (2.41) by constructing an iterative minimisation procedure, within each iteration of which a linear problem is solved to find $\mathbf{q}$. We use the $MATLAB$ optimisation routine *lsqnonlin* for the iteration of the minimisation procedure, and at each iteration we make use of the L-curve criterion from the linear inverse theory to estimate the regularisation parameter. However, by experiment we found that this approach leads to an oscillation in values of λ, as shown in Figure 30, and most of the time the approach does not give the desired solution. To overcome this problem we solve the solution process by fixing the value of λ at each iteration.

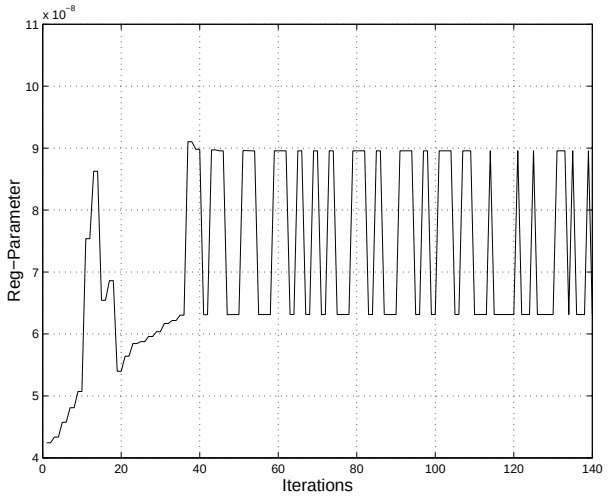

Figure 30: Use of linear L-curve for nonlinear problem

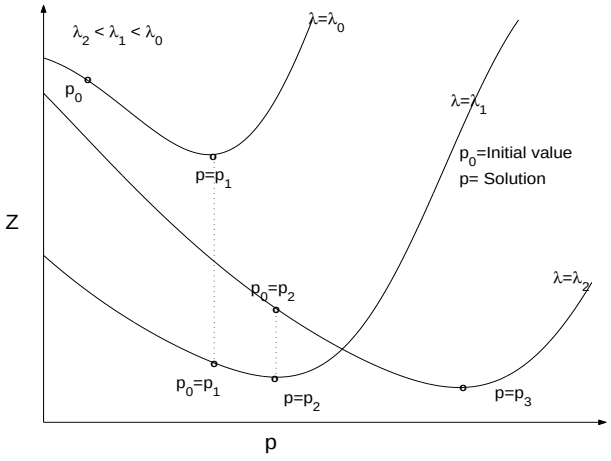

Figure 31: 1-D illustration of the minimization of function

3.2 Method 2- fixed λ

First, we introduce an L-curve intended for the non-linear problem (2.41). We will call this the non-linear L-curve. The idea is to compute the solution path displaying norm of the linear solution against the residual norm for a sequence of λ values. The short algorithm for computing the L-curve goes as follows:

(i) carry out steps (ii) and (iii) for a sequence of λ values, as illustrated in Figure 31;

(ii) solve (2.41) using *MATLAB*'s optimisation routine *lsqnonlin* for a fixed value of λ;

(iii) take the solution $\mathbf{p}$ from the previous step as an initial value to the next problem with a new λ (see Figure 31);

(iv) plot the curve of residual norm $\log \|A\mathbf{q} - \mathbf{c}\|$ *vs* solution norm $\log \|L\mathbf{q}\|$.

This curve also exhibits a corner (see Figure 32a). As the regularisation parameter decreases towards the corner, the solution norm changes very little, while the error norm is reduced to a comparatively large extent. A decrease of the regularisation parameter further than the corner results in larger increases in the solution norm, with very little decrease in the error norm.

Method 2a Maximum curvature

Numerically, the point of maximum curvature of the curve locates the corner. Figures 32a and b illustrates the procedure. Figure 32a is the non-linear L-curve where the corner is clearly indicated and Figure 32b is the curvature of the L-curve as a function of λ. The peak in Figure 32b corresponds to the corner of the L-curve. The corner is defined as the point on the L-curve:

$$(\varsigma(\lambda), \zeta(\lambda)) = (\log \|A\mathbf{q} - \mathbf{c}\|, \log \|L\mathbf{q}\|) \tag{3.44}$$

with maximum curvature. Here the curvature k is defined as:

$$\kappa(\lambda) = \frac{\varsigma' \zeta'' - \varsigma'' \zeta'}{((\varsigma')^2 + (\zeta')^2)^{\frac{3}{2}}} \tag{3.45}$$

where the differentiation is with respect to λ. Unlike the linear problem, the non-linear objective Z may have more than one minimum for each value of λ and this leads to several non-linear L-curves. Therefore, the solution process of (2.41) should include

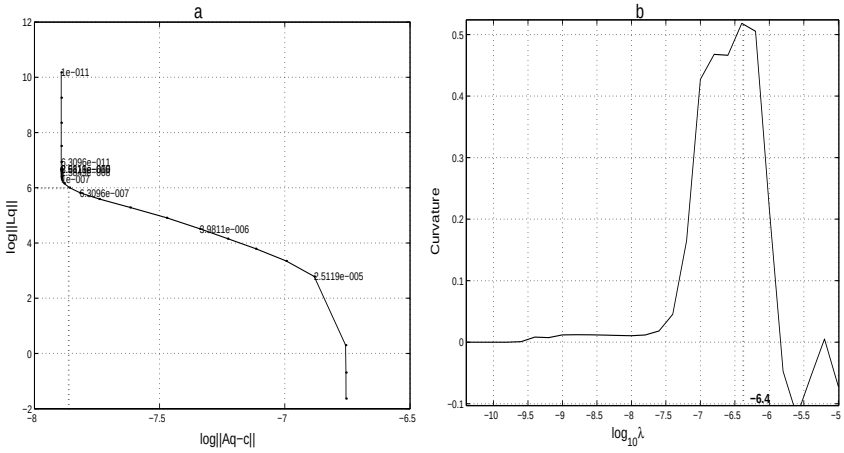

Figure 32: This figure demonstrates the use of maximum curvature method to estimate the optimal value of a regularisation parameter: (a) non-linear L-curve, (b) regularization parameter *vs* curvature

(i) finding all L-curves,

(ii) finding the best optimal point on the L-curves.

To deal with these problems we have developed an algorithm to determine the best L-curve and its corner.

The Parameter Estimation Algorithm -1

Let us now consider the numerical details of the algorithm to solve (2.41). The solution is arrived at through three steps. In the first step, we find all or most of the local minimum of (2.41) for a fixed value of λ when it is equal to its lowest value in the sequence. This is done by solving (2.41) many times, at each time with a different initial value $\mathbf{p} = \mathbf{p}_0$. We choose $\mathbf{p}_0$ randomly using the $MATLAB$ function *rand* within a selected interval. There is one important reason for solving (2.41) for a fixed lowest λ. Equation (2.41) contains the error norm (ϕ_d) and the solution norm (ϕ_m) where the first is a non-linear part and the later is quadratic. Therefore, (2.41) is almost quadratic if λ is large, and non-linear if λ is small. We also found that the number of local minima of (2.41) increases with the decreasing values of λ. Therefore the number of local minima of Equation (2.41) for the lowest value of λ identifies all or most (say n_l) of the L-curves for this equation.

In the second step, we take each of the local minima obtained from the first step as the starting value to solve (2.41) for a sequence value of λ from lowest to largest. That means solving (2.41) n_l (number of local minima when λ is equal to its lowest value) times for a sequence values of λ. The idea behind this is to compute all or most of the L-curve displaying the error norm (or data misfit) versus the solution norm for a sequence values of λ. One such example is shown in Figure 36a.

The third and final step is to pick the optimal point on each curve and then select the best among those. The optimal point on each curve is calculated by examining the curvature along the L-curve. This can also be calculated using the rotated L-curve or NGCV methods that are described in the next subsections.

Method 2b- Non-linear GCV

Here we adapt Wahhba's (20) 'leaving-out-one' lemma to our non-linear problem. This lemma is based on the idea of removing one of the data points (c_i) from a given array of data $\mathbf{c}$ and then solving (2.41) using all the remaining data. The resulting inverse solutions $\mathbf{p}$ and $\mathbf{q}$ will predict the right hand vector $\mathbf{c}$, which can be used to estimate the omitted element c_i. Let the error in the misfit be equal to $\|c_i - \hat{c}_i\|$, where $\hat{c}_i$ is the estimated value. For a fixed value of λ, we repeat this process n times (number of data points) and sum the error misfits. We then have

$$\sum_{i=1}^{n} (c_i - \hat{c}_i)^2 .$$

If we repeat the whole process for a sequence of λ values, we then have the function

$$V(\lambda) = \sum_{i=1}^{n} (c_i - \hat{c}_{\lambda i})^2 .$$

The best value of λ can then be defined as the one that gives the smallest sum of misfits. We

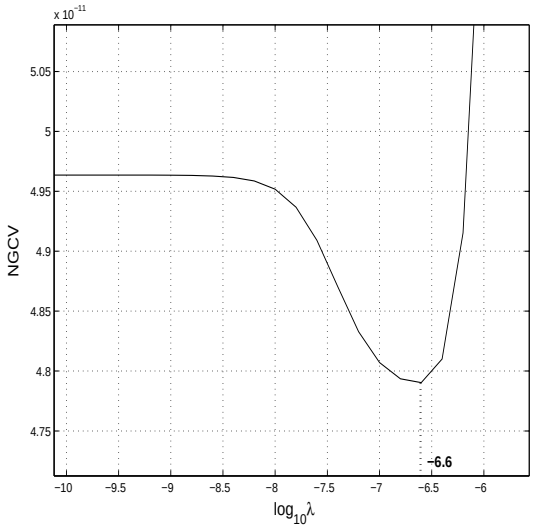

Figure 33: parameter selection- NGCV method

will call this method the NGCV. Computationally, NGCV is very expensive. The basic approach behind the NGCV and the GCV is the same. The GCV defined in our previous paper (12) is for linear problem where the matrix A is same for all values of λ but in the non-linear problem A is a function of $\mathbf{p}$. Therefore we cannot use GCV directly to estimate the optimal value of λ. Figure 33 shows the estimation of λ using NGCV method for the same simulated data considered in the last subsection, where the lowest value of NGCV function is clearly indicated. The maximum curvature method and NGCV method use different approaches and therefore, each method will in general find a different optimal value of λ. Computationally, the maximum curvature method is much cheaper than NGCV.

Method 2c Rotated L-curve

The optimal point on the L-curve can also be detected by another simple method (6), (5) which proceeds by defining the rotated L-curve (see Figure 34):

$$\psi(\theta) = \tau + \zeta, \qquad \theta = \tau - \zeta \tag{3.46}$$

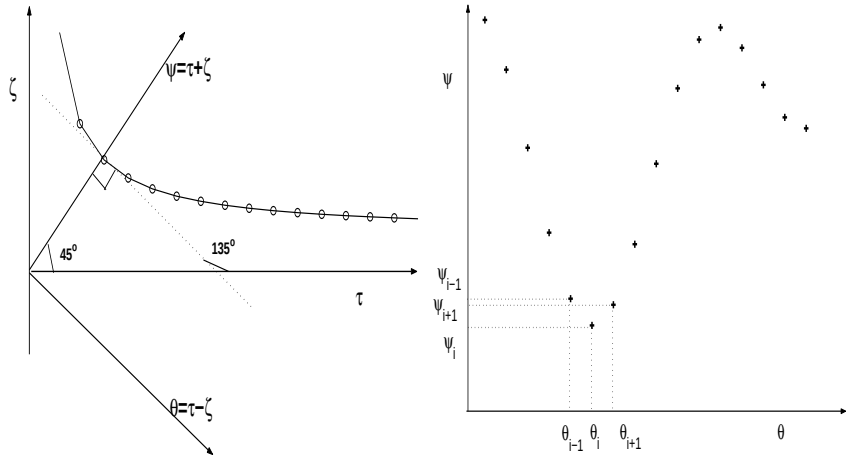

Figure 34: Rotation of L-curve

where $\tau = \log \|A(\mathbf{p})\mathbf{q} - \mathbf{q}\|$ is the error norm function and $\zeta = \log \|L\mathbf{q}\|$ is the solution norm function. Then, any three neighbouring points

$$(\theta_j, \psi_j)\,, j = 1, \ldots, n \tag{3.47}$$

will define a parabola. If $\psi_{j-1} > \psi_j$, $\psi_j < \psi_{j+1}$ for any j, then ψ_j will be a candidate for minimum ψ. The value of λ corresponding to ψ_j may be used as an approximation to an optimal value of the regularisation parameter. Figure 35a shows the rotated L-curve of Figure 32a. It can be seen clearly that none of the points on the curve had formed a parabola. This is because of the dominance of the solution norm over the error norm. This difficulty can be overcome by scaling the axis. But the main problem here is to find the exact value for the scaling factor. Rotated L-curves for different scaling factors are shown in Figure 35. It shows that the estimated optimal λ varies slightly with the different scaling factor. It is very hard to calculate the exact scaling factor, only an approximate value of the scaling factor can be obtained from the L-curves. Therefore optimal λ obtained using rotated L-curve method described in this section is only a rough approximation. Alternatively, the corner can be located using the derivative of the L-curve. At the corner, the derivative of the L-curve is approximately equal to -1, i.e. the angle between the tangent at the corner and the + ve axis of the data misfit function τ is 135 °. But in our problem magnitude of the solution norm is much larger than the error norm and therefore at the corner the value of the derivative does not have to be -1 unless we use the exact scaling.

The Table 8 shows the comparison of the optimal value of λ obtained for the non-linear L-curve shown in Figure 32a using different methods described in this section.

Table 8: Comparison of parameter selection methods

Method	λ
Maximum curvature	3.9811×10^{-7}
NGCV	2.5119×10^{-7}
Rotated L-curve	
scale 1:14	1.5849×10^{-7}
scale 1:12	2.5119×10^{-7}
scale 1:8	2.5119×10^{-7}
scale 1:1	none

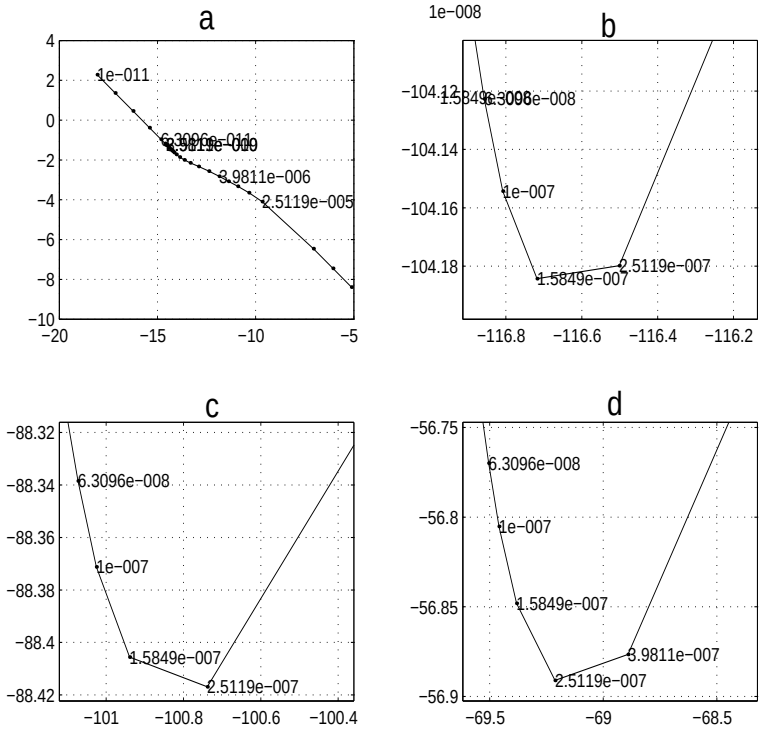

Figure 35: Rotated L-curves: (a) scaling factor=1, (b) scaling factor=14, (c) scaling factor=12, (d) scaling factor=8

Difficulties

Now consider the example given in Figure 36. All L-curves and their respective corners are clearly shown in Figure 36a. Figures 36b and c are the log of the norm of the error in **p**, **q** against log of λ respectively. Figure 36d is the error norm of the L-curves against log of λ. From Figures 36b, c and d it can be seen that the corner (L-curve 3) with the smallest error norm gives the lowest error in the **p** and **q** estimates than other corners. This criterion works well. However, with some extensive simulations, we found that roughly one out of four failures occurs. Figure 37 shows the example in which the criterion selects a bad corner, P_1, on the L-curve-1. Figure 37a shows all the L-curves and their corners. P_1 is the corner on the L-curve-1, P_2 and P_3 are the corners on the L-curve-2. Here we used the maximum curvature method to locate the corners. Relative error measures in **p** and **q** are shown in Figures 37b and c respectively in a log scale. These figures clearly shows that the error in **p** and **q** estimates at the corner P_3 is smaller than the errors at the corners P_1 and P_2. Therefore the corner P_3 should be the better choice than other corners but the criterion we use failed to locate P_3. To overcome these problems we have slightly modified our present algorithm to determine the best L-curve and its corner

The Parameter Estimation Algorithm-2

Let us now consider the numerical details of the algorithm to solve (2.41). The solution is arrived at through four steps. First two steps are similar to the previous algorithm. The idea behind the first two steps is to compute all or most of the L-curve displaying the error norm (or data misfit) versus the solution norm for a sequence values of λ. One such example is shown in Figure 38 by

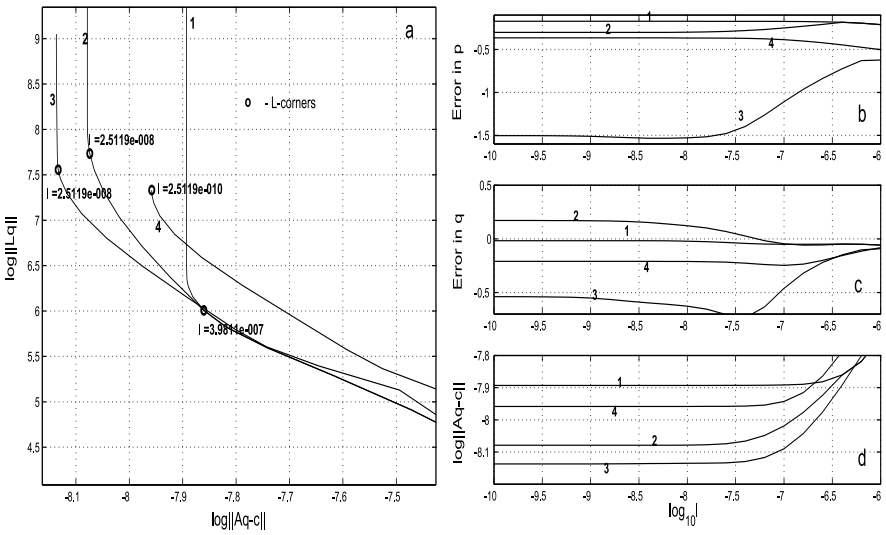

Figure 36: Good example: (a) non-linear L-curves, (b) relative error in **p** *vs* regularisation parameter, (c) relative error in **q** *vs* regularisation parameter, (d) data misfit *vs* regularisation parameter

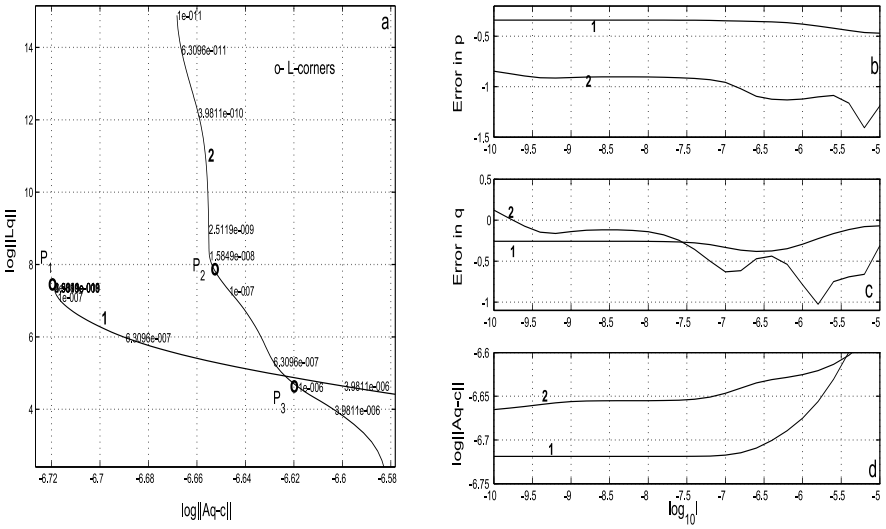

Figure 37: Bad example: (a) non-linear L-curves, (b) relative error in **p** *vs* regularisation parameter, (c) relative error in **q** *vs* regularisation parameter, (d) data misfit *vs* regularisation parameter

dashed lines. In the third step, for each λ, we pick a point that gives the lowest function value to construct the final L-curve. Finally, we smooth the L-curve on a log-log scale by a spline curve similar to the work done by Hansen (9). It is shown by the solid thick line in Figure 38. The fourth and final step is to pick the optimal point on the curve. This can be calculated either by using the rotated L-curve or by examining the curvature along the L-curve or NGCV method.

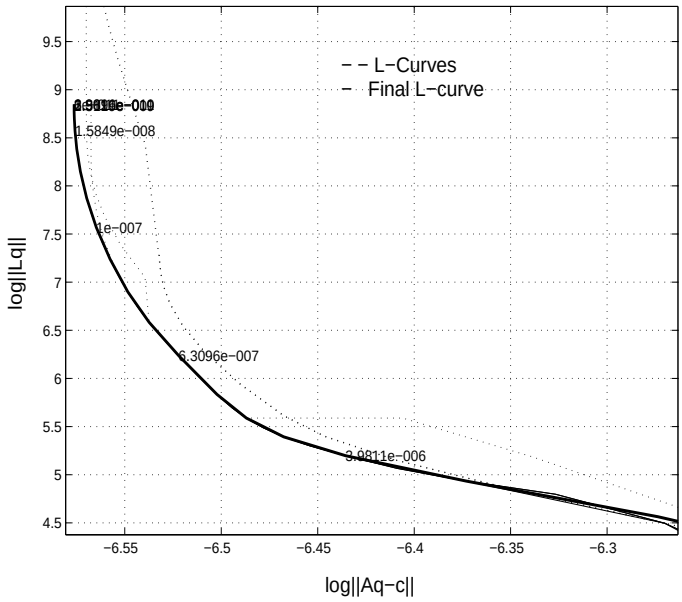

Figure 38: L-curves

3.3 Method 3 - fixed λ (Cheaper Method)

In this section, we build up an algorithm as a cheaper alternate to the method 2. The inspiration behind this algorithm is based on the work of (2), (3). In this work, the optimal λ value of the nonlinear minimisation problem

$$\begin{aligned} \min_{\mathbf{x}} \ \phi(\mathbf{x}) &= \|F(\mathbf{x}) - \mathbf{c}\|^2 + \lambda^2 \|L\mathbf{x}\|^2 \\ &= \phi_d(\mathbf{x}) + \lambda^2 \phi_m(\mathbf{x}) \end{aligned} \tag{3.48}$$

is projected using linear inverse theory (L-curve or GCV). In 3.48, ϕ_d is an error norm, ϕ_m is a solution norm and λ is a regularisation parameter that balances the two components. In this problem the relationship between the data and the parameters $\mathbf{x}$ is non-linear. The non-linear relationship is overcome by constructing an iterative procedure in which the non-linear minimisation problem is replaced at each iteration by its linearised approximation. Differentiation of (3.48) with respect to $\mathbf{x}$ and equating the result to zero gives

$$\frac{\partial \phi}{\partial \mathbf{x}} = \lambda^2 L^T L\mathbf{x} + J(\mathbf{x})^T \left(F(\mathbf{x}) - \mathbf{c}\right) = 0, \tag{3.49}$$

where $J(\mathbf{x}) = \frac{\partial F}{\partial \mathbf{x}}$. Then we linearsed (3.49) by

$$\lambda^2 L^T L(\mathbf{x} + \delta\mathbf{x}) + J(\mathbf{x})^T \left(F(\mathbf{x}) + J(\mathbf{x})\delta\mathbf{x} - \mathbf{c}\right) = 0.$$

At the n-th iteration, we solve the linear system of equation for $\delta\mathbf{x}$ is

$$\left(J(\mathbf{x_n})^T J(\mathbf{x_n}) + \lambda^2 L^T L\right) \delta\mathbf{x} = J(\mathbf{x_n})^T \left(\mathbf{c} - F(\mathbf{x_n})\right) - \lambda^2 L^T L\mathbf{x_n}. \tag{3.50}$$

By letting $\mathbf{x_n} = \mathbf{x_{n-1}} + \delta\mathbf{x}$, (3.50) gives

$$\left(J(\mathbf{x_{n-1}})^T J(\mathbf{x_{n-1}}) + \lambda^2 L^T L\right) \mathbf{x_n} = J(\mathbf{x_{n-1}})^T \left(\mathbf{c} - F(\mathbf{x_{n-1}})\right) + J(\mathbf{x_{n-1}})\mathbf{x_{n-1}}.$$

This problem is identical to the linear least squares problem

$$\begin{bmatrix} J(\mathbf{x_{n-1}}) \\ \lambda L \end{bmatrix} \mathbf{x_n} = \begin{bmatrix} c - F(\mathbf{x_{n-1}}) + J(\mathbf{x_{n-1}})\mathbf{x_{n-1}} \\ 0 \end{bmatrix}. \tag{3.51}$$

At the n-th iteration, we solve the linear least squares problem (3.51). In the development of the solution, the value of λ starts from a larger value and then decreases from one iteration to the next slowly in conjunction with the equation

$$\lambda_{n+1} = \max(c\lambda_n, \lambda^*), \tag{3.52}$$

where $0.01 \leq c \leq 0.5$, λ^* is an optimal value of regularisation parameter obtained either using the linear L-curve or GCV at the n-th iteration for the linear problem (3.51), and λ_n, λ_{n+1} are the values of λ at n-th, $(n+1)$-th iteration, respectively. The Equation (3.52) efficiently imposes a steady decrease on λ values and giving consistent algorithm for the non-linear inverse problem. Iteration is carried out until λ, the error norm and the solution norm all have steady state. At steady state, optimal value of regularisation parameter, λ^*, obtained using L-curve (or GCV) for the linear problem (3.51) is equal to the final λ value. i.e. $\lambda^* = \lambda_{n+1}$. It has been demonstrated (2), (3) (10) using simulated data sets that at the final iterations the obtained value of regularisation parameter was a good estimate of what was expected for a given noise level in the data.

Difficulties

Here, we propose the above approach of estimating optimal λ to our problem (2.41). The idea is to solve (2.41) for a sequences of λ's (each λ acts as the only regularisation parameter for the problem) so that this sequence approaches a steady state as it proceeds. This algorithm is as follows:

1. Choose the starting point $\mathbf{p} = \mathbf{p_0}$, index $I = 1$, and initial value of regularisation parameter $\lambda_I = \lambda_0$, which is very large.
2. Until convergence of λ, $\|A(\mathbf{p})\mathbf{q} - \mathbf{c}\|$, $\|L\mathbf{q}\|$ do
   (i) solve (2.41) for fixed λ_I, and find the solution $\mathbf{p} = \mathbf{p_I}$;
   (ii) obtain the optimal value of $\lambda = \lambda^*$ for the linear problem
   $$\min_{\mathbf{q}} \ \|A(\mathbf{p_I})\mathbf{q} - \mathbf{c}\| + \lambda^2 \|L\mathbf{q}\|$$
   using the linear L-curve;
   (iii) update the λ value, $\lambda_{I+1} = \max(c\lambda_I, \lambda^*)$;
   (iv) take the solution $\mathbf{p_I}$ as the starting point to the next problem with $\lambda = \lambda_{I+1}$;
   (v) I=I+1.

By numerical experiments we have found that this approach does not lead to our desired solution. In order to better explain this, we provide the non-linear L-curves (solution curve or path) of (2.41). When λ is small, the solution of (2.41) may have several local minima and this leads to several non-linear L-curves, as shown in Figure 39. Suppose that curve 1 is the path of global minimal solution to (2.41), and curves 2, 3 and 4 are the corresponding local minimal solutions for various λ values. The value of λ at M is large and therefore gives only one minimum for (2.41). If we start from M, there is no guarantee the solution path of (2.41) will be curve 1 in Figure 39. It might be curves 2 or 3 or 4 in Figure 39. This example clearly demonstrates that the above approach is not very useful for our problem. To overcome the difficulty, we have to modify this approach slightly.

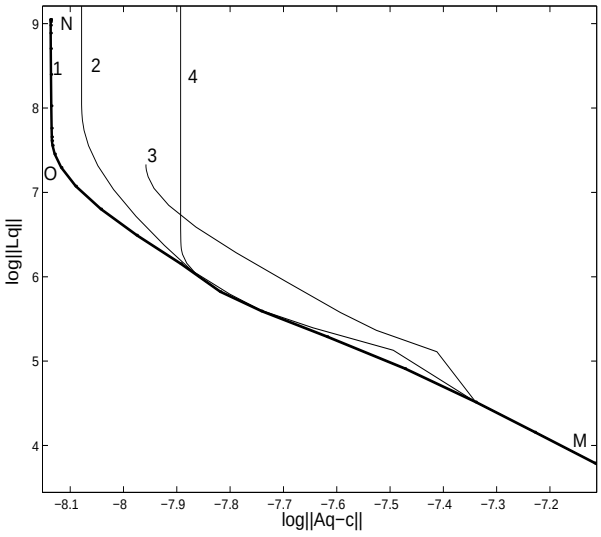

Figure 39: Non-linear L-curves

The Modified Method

Here, we propose a new methodology for solving (2.41). The approach is similar to the above algorithm given in section 6.3.3, but here we start with a small regularisation parameter and then slowly increase its value. In the first step, we find all or most of the local minima of (2.41) for the starting value of λ. At this stage we have to be very careful to avoid rank deficiency when we choose a small value of λ.

In the second step, we take each of the local minima obtained from the first step as the starting value to solve (2.41) for various λ from small to large. We increase λ slowly using the formula $\lambda_{I+1} = \min(c\lambda_I, \lambda^*)$, where $c > 1$, λ^* is the optimal value of the regularisation parameter obtained using linear L-curve for the sub-problem

$$\min_{\mathbf{q}} \ \|A(\mathbf{p_I})\mathbf{q} - \mathbf{c}\| + \lambda^2 \|L\mathbf{q}\|,$$

and $\mathbf{p}_I$ is the global minimal solution for λ_I. We repeat this process until λ, the error norm and the solution norm have achieved steady state (or convergence). When c is small, it takes a longer time to converge on λ, but the gap between two points on the minima solution curves are close enough and it therefore avoids jumping from one curve to other (see Figures 40a & b). Therefore use of a small value for c is recommended. A sample solution path of minimisation problem (2.41) is shown in the Figure 41. From this figure it is clear that some of the work done using the method described in section 6.3 is a waste. Therefore the method described in this section is computationally more efficient (cheaper) than the previous method. Both methods are safer since we increase λ slowly, and for each λ we find all local minima and select the minimal solution that gives the objective function minimum. Therefore, there is no way to trap in a local minimum. These two methods use different approaches to approximate the optimal value, and therefore each method may find different optimal value of λ.

4 Confidence Interval Estimation

A confidence interval uses sample data to estimate an unknown parameter with an indication of how accurate the estimate is and of how confident we are that the result is correct. In this section,

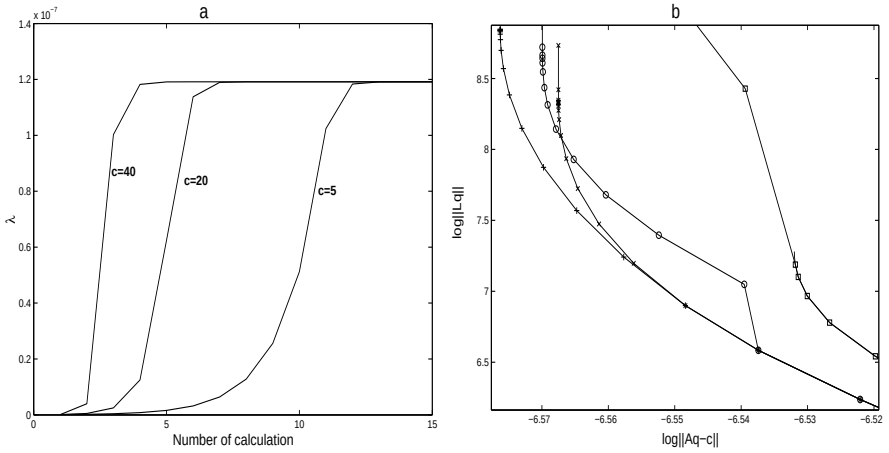

Figure 40: (a) Convergence of λ for different values of c, (b) minima solution paths

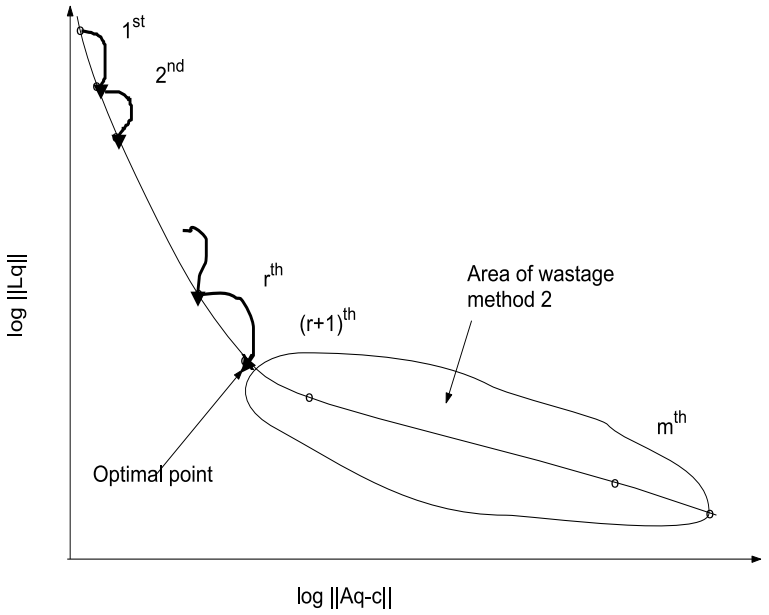

Figure 41: Nonlinear solution path

we will develop a method of constructing confidence intervals for the non-linear ill-posed problem given in (2.41). Let

$$\mathbf{z} = [\mathbf{q}, \mathbf{p}]^T, \ \mathbf{p} = [X_0, Y_0, H]^T, \ \mathbf{q} = [q_1, q_2, \ldots, q_m]^T.$$

The estimate of the variance-covariance matrix of $\hat{\mathbf{z}}$ is given by (**?**)

$$var(\hat{\mathbf{z}}) = s^2 \left(W^T W\right)^{-1}, \tag{4.53}$$

where $\mathbf{W} = [A \ J]$ is the matrix of partial derivatives of $\mathbf{c}$,

$$J_{ij} = \sum_j \frac{\partial A_{ij}}{\partial (X_0, Y_0, H)} q_j,$$

and s^2 is the residual mean square given by

$$s^2 = \sum_{i=1}^{n+1} \frac{[C_i - A(\hat{\mathbf{p}})\hat{\mathbf{q}}]^2}{n+1-r},$$

here r is the length of the vector $\mathbf{z}$. Since the least-squares problem given in (2.40) is ill-posed, we should therefore include regularisation in computing the confidence intervals. We only use the regularisation to calculate the linear parameters. If we assume

$$\mathbf{f}(\mathbf{z}) = A(\mathbf{p})\mathbf{q},$$

then (2.41) can be written as

$$\min_{\mathbf{z}} \left[\|f(\mathbf{z}) - \mathbf{c}\|^2 + \lambda^2 \| \begin{bmatrix} L & 0 \end{bmatrix} \begin{bmatrix} \mathbf{q} \\ \mathbf{p} \end{bmatrix} \|^2 \right]. \tag{4.54}$$

Therefore the variance-covariance matrix of $\hat{\mathbf{z}}$ with regularisation is

$$var(\hat{\mathbf{z}}) = s^2 \left(w^T w\right)^{-1}, \quad w = \begin{bmatrix} W \\ \lambda \begin{bmatrix} L & 0 \end{bmatrix} \end{bmatrix}.$$

The standard error of $\mathbf{z}$ can be calculated by computing the square roots $\mathbf{z_{sq}}$ of the diagonal elements of $s^2(w^T w)^{-1}$ (**?**). Confidence interval estimations are based on the t-distribution, e.g., 95% confidence interval is in the form of $\mathbf{z} \pm t_{.025}\mathbf{z_{sq}}$.

5 Modelling Applications

In this section, we present numerical calculations to evaluate the accuracy of the methods developed. To do so, we consider an input of concentration data generated from a point source of strength $q(t)$ kg s^{-1} located at $(0, 0, H)$ in the Cartesian coordinate system. We simulate the concentration signals at downstream locations $P = (X_0, Y_0, 0)$, $Q = (X_0 + 30, Y_0 + 30, 0)$ and $R = (X_0 + 100, Y_0 + 70, 0)$ for all examples except Example 5 in this section. In Example 5, distances between source and measurement locations are very large compared with other examples, and we therefore simulate concentration signals at downstream locations $P = (X_0, Y_0, 0)$, $Q = (X_0 - 300, Y_0 - 30, 0)$ and $R = (X_0 + 200, Y_0 + 70, 0)$. We obtain concentration signals by using the forward problem (2.37) and true parameter values. In order to simulate errors, we corrupt the concentration signals by adding normally distributed random noise. For illustrative purposes, K_x, K_y, K_z and U are taken as 12, 12, 0.2113 and 1.8, respectively.

5.1 Method 2

We consider five examples to demonstrate the developed method for finding the release rate $q(t)$ and the location (X_0, Y_0, H) using method 2. The purposes of these examples are:

(i) to demonstrate the simultaneous estimation of parameters X_0, Y_0, H, and the source release function $q(t)$;

(ii) to demonstrate the accuracy of the method to handle different situations such as noise in the data, source type, the discretisation size of the source function, larger distances between source and measurement points, and so on.

Example 1: Measured data corrupted by 10% of two different types of random noise

In this example we consider two sets of data where each set is corrupted by 10% of different random noise. The results of the source-term estimation are summarised in Table 9, and Figures 42 and 43. Listed in Table 9 are the true non-linear parameter (location) values along with the reconstructed (or estimated) values and their confidence intervals. The L-curve that has lowest function value is shown in Figures 42a and 43a. Figures 42b–43b are the curvature of the L-curves as a function of λ. The peaks in the figure correspond to the corners on the respective L-curves (P_1 & P_2 in Figure 42a, and P_1 & P_3 in Figure 43a). The Figures 42c and 43c illustrate the NGCV method to estimate the optimal point on the L-curve, where the lowest value of the NGCV function is clearly indicated (P_3 is a corresponding point in Figure 42a, and P_2 is a corresponding point in Figure 43a). Figures 42d and 43d depict the true error in the solution as a function of λ. Here, the true error refers to the difference between the reconstructed and simulated (perfect) concentration values. This plot is only possible if we know the true concentration. Figures 42e and 43e depict the error in **q** (release rates) as a function of λ. Figures 42f and 43f depict the error in the reconstructed location **p** as a function of λ.

Table 9: Example 1: Different random noise of 10% in the measured signal

		data 1	data 2
p	True value	Estimated value ± Confidence interval	
X_0	150.00	162.00 ± 9.42	153.20 ± 10.16
Y_0	25.00	19.3 ± 6.83	21.00 ± 8.21
H	12.00	11.1 ± 0.85	11.75 ± 0.72

For the first set of data, P_1, P_2 and P_3 are the three possible candidates for the optimal point on the L-curve (Figure 42a), and the points O_1, O_2 and O_3 respectively (Figure 42d) are their corresponding true errors. O_0 is the point where the true error is minimum. The point O_1 is closer to the minimum O_0 than the other two points, and therefore the regularisation parameter corresponding to a point O_1 is more suitable value for the problem than other values. Similarly for the second set of data, the three candidates are P_1, P_2, P_3 (Figure 43a) and the points O_1, O_2 and O_3 respectively (Figure 43b) are their corresponding true errors. O_1 is closer to the minimum than other two points, and therefore the regularisation parameter corresponding to point O_1 is more suitable value for the problem than other values.

It can be seen from Figures 42d and 43d that (i) the true errors are not exactly same and the minimum occurred at two different values of λ, (ii) in both cases the error in the reconstructed solution is dominated by regularisation rather than by noise in the data since the estimated optimal points lie on the right of the true minimum, and (iii) the error in the solution for the first data set is larger than for the second data set. Since both data sets are corrupted by the same size of noise, we can therefore conclude that the error in the reconstructed solution depends on the data pattern (randomness).

Example 2: Measured data corrupted by the different size of the same random noise

In this example we consider four sets of data: perfect data, and data corrupted by 1%, 5% and 10% of the same random noise. Twenty data samples are taken between the times t=0.01 and t=300, and the release rate function is discretised into ten equal parts over the same time interval. The results of the source term estimation are summarised in Table 10 and Figures 44–47. Listed in the Table 10 are the true non-linear parameter (location) values along with the reconstructed values and their confidence intervals. The L-curve, which contains the function minimum, is shown in Figures 44a–47a for each data set. Figures 44b–47b are the curvature of the L-curve as a function of λ. The peaks in each figure correspond to the corner on the corresponding L-curves (P_1 in

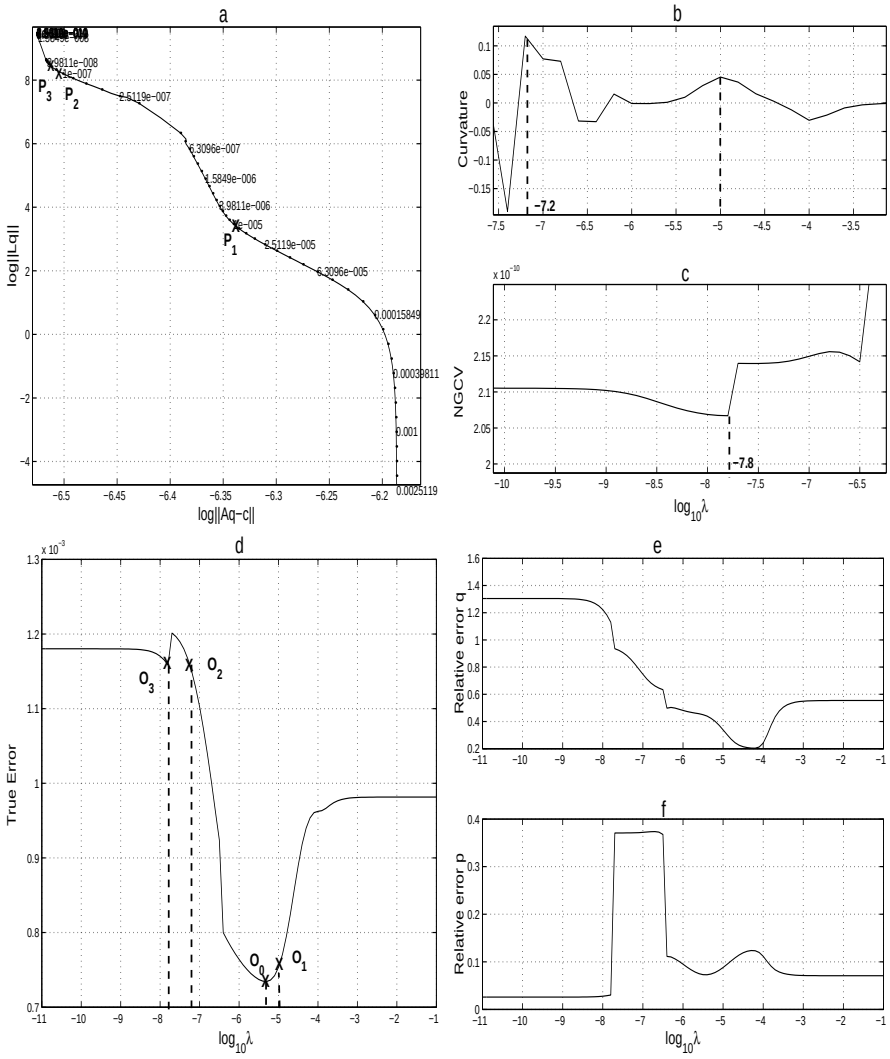

Figure 42: Example 1- data 1: (a) non-linear L-curve, (b) curvature *vs* regularisation parameter, (c) NGCV *vs* regularisation parameter, (d) true error *vs* regularisation parameter, (e) relative error in **q** *vs* regularisation parameter, (f) relative error in **p** *vs* regularisation parameter

Figure 44a, 45a, 47a and P_1, P_2 in Figure 46a). Figures 44c–47c illustrate the NGCV method to estimate the optimal point on the L-curve, where the lowest value of the NGCV function is clearly indicated. The point P_2 is their corresponding point on the L-curve in Figures 45a, 47a, and P_3 is in Figure 46a. In Figure 44c, the minimum of the NGCV function is very flat and therefore it is not possible to locate the minimum. Figures 44d–47d depict the true error in the solution against regularisation parameter. Figures 44e–47e depict the true linear parameter (release rates), along with its reconstructed value and confidence interval.

For the first set of data, P_1 is the only candidate for the optimal point on the L-curve (Figure 44a), and the point O_1 (Figure 44b) is its corresponding true error. The error at the point O_1 is not zero, even though the data are exact. This shows the effect of regularisation on the accuracy of the solution. For the second set of data, P_1 and P_2 are the candidates for the optimal point on the L-curve (Figure 45a), and the points O_1, O_2 (Figure 45b) are their corresponding true errors. Here

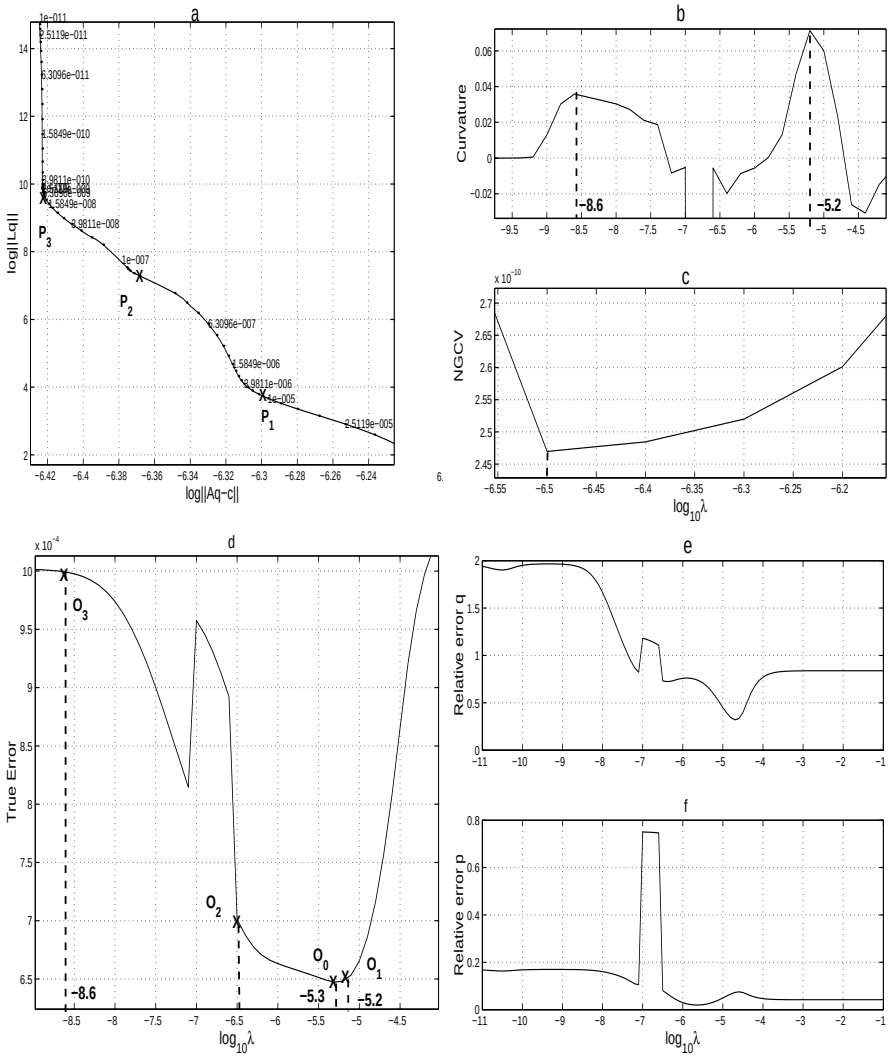

Figure 43: Example 1- data 2: (a) non-linear L-curve, (b) curvature *vs* regularisation parameter, (c) NGCV *vs* regularisation parameter, (d) true error *vs* regularisation parameter, (e) relative error in **q** *vs* regularisation parameter, (f) relative error in **p** *vs* regularisation parameter

the point O_1 is our choice, since it is closer to the true minimum (O_0) than O_2. The error at O_1 is larger than the true minimum and is on the right of O_0 (true minimum), i.e. the regularisation error dominates rather than the noise in the total error. For the third set of data, P_1, P_2 and P_3 are the candidates for optimal points on the L-curve (Figure 46a), and the points O_1, O_2 and O_3 (Figure 46d) are their corresponding true errors. The point O_1 is closer to the true minimum (O_0) than other two points and therefore the regularisation parameter corresponding to the point P_1 is more suitable value for the problem than other values. The error at point P_1 is larger than the true minimum, and is on the left side of O_0 (true minimum). This shows that the total error term is dominated by the noise in the data. Finally, for the fourth set of data, P_1 and P_2 are the candidates for optimal points on the L-curve (Figure 47a), and the points O_1 and O_2 (Figure 47d) are their corresponding true errors. The point O_1 is our choice, since it is closer to the true minimum than O_2. The error at point O_1 is larger than the true minimum (O_0), and is on the left

Table 10: Case 2: Different size of same random noise (0%, 1%, 5%, and 10%) in the measured signal

		Noise in the data			
		0%	1%	5%	10%
p	True value	Estimated value ± Confidence interval			
X_0	200.00	202.33 ± 0.37	202.73 ± 2.0	206.5 ± 8.65	183.6 ± 19.20
Y_0	30.00	30.2 ± 0.05	31.2 ± 1.70	34.2 ± 5.49	37.15 ± 9.80
H	10.00	9.98 ± 0.01	10.09 ± 0.09	10.65 ± 0.51	10.95 ± 0.75

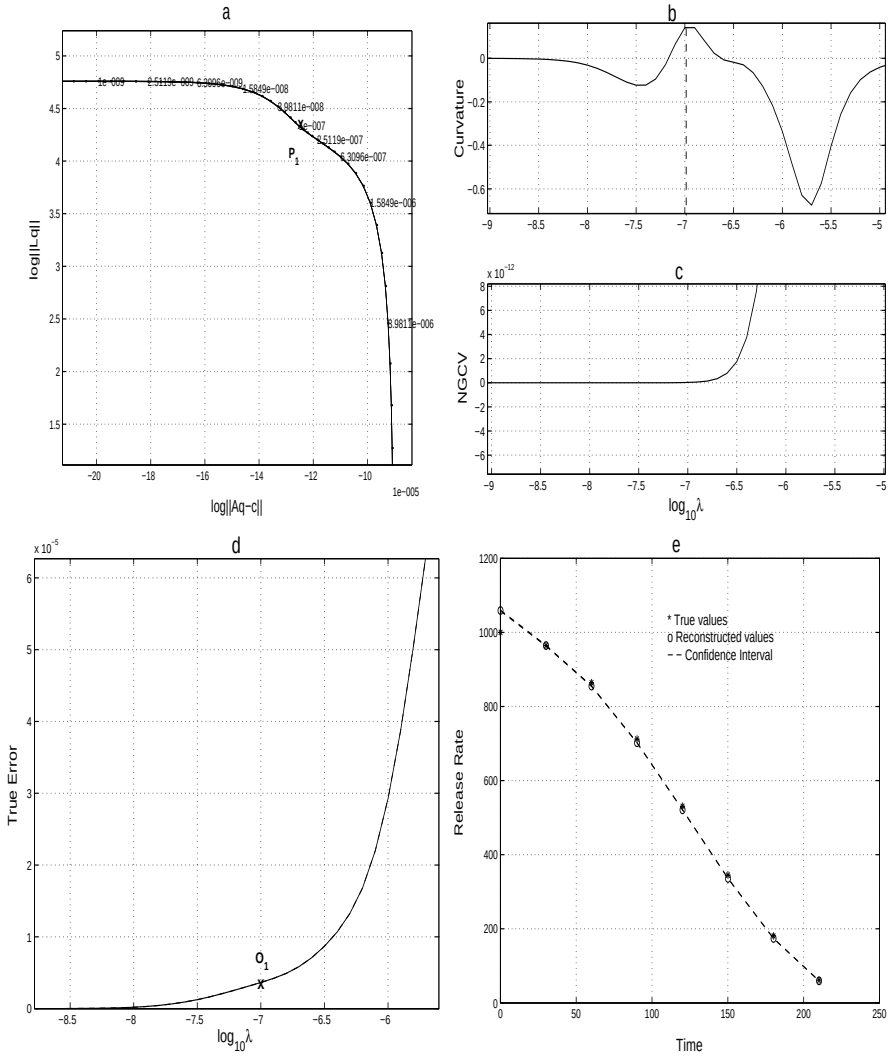

Figure 44: Example 2- data 1: (a) non-linear L-curve, (b) curvature *vs* regularisation parameter, (c) NGCV *vs* regularisation parameter, (d) true error *vs* regularisation parameter, (e) release rates *vs* time

side of O_0 (true minimum). This shows the total error term is dominated by the noise in the data.

It can be seen from Figures 44–47 that (i) the true error increases with increasing noise in the

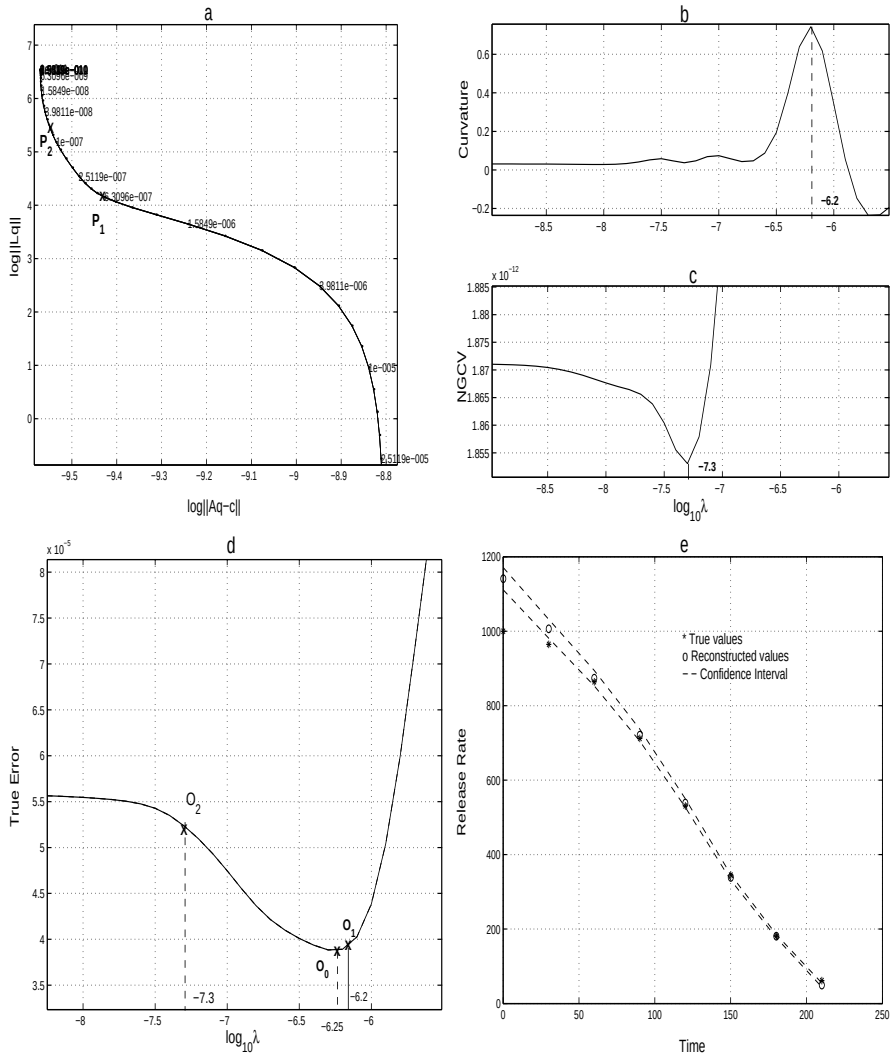

Figure 45: Example 2- data 2: (a) non-linear L-curve, (b) curvature *vs* regularisation parameter, (c) NGCV *vs* regularisation parameter, (d) true error *vs* regularisation parameter, (e) release rates *vs* time

data, (ii) the size of the confidence interval increases with increasing noise in the data, (iii) the errors in the first two reconstructed solutions are dominated by the regularisation error, while the last two are dominated by noise in the data.

Example 3: Different numbers of source points m, data points n

In this example we consider the first three of the four data sets from the previous example. Twenty data samples are taken over the time interval $t_0 = 0.01$ to $t_n = 300$, and the release-rate function is discretised into fifteen equal parts over the same time interval. The results of the source-term estimation are summarised in Table 11, Figures 48–50. Listed in the table are the true non-linear parameter (location) values along with the reconstructed values and confidence interval estimates. The L-curves, which have function minimum, are shown in Figures 48a–50a for each set of data. Figures 48b–50b depict the error in the linear parameters (release rates) as a function of λ. Figures

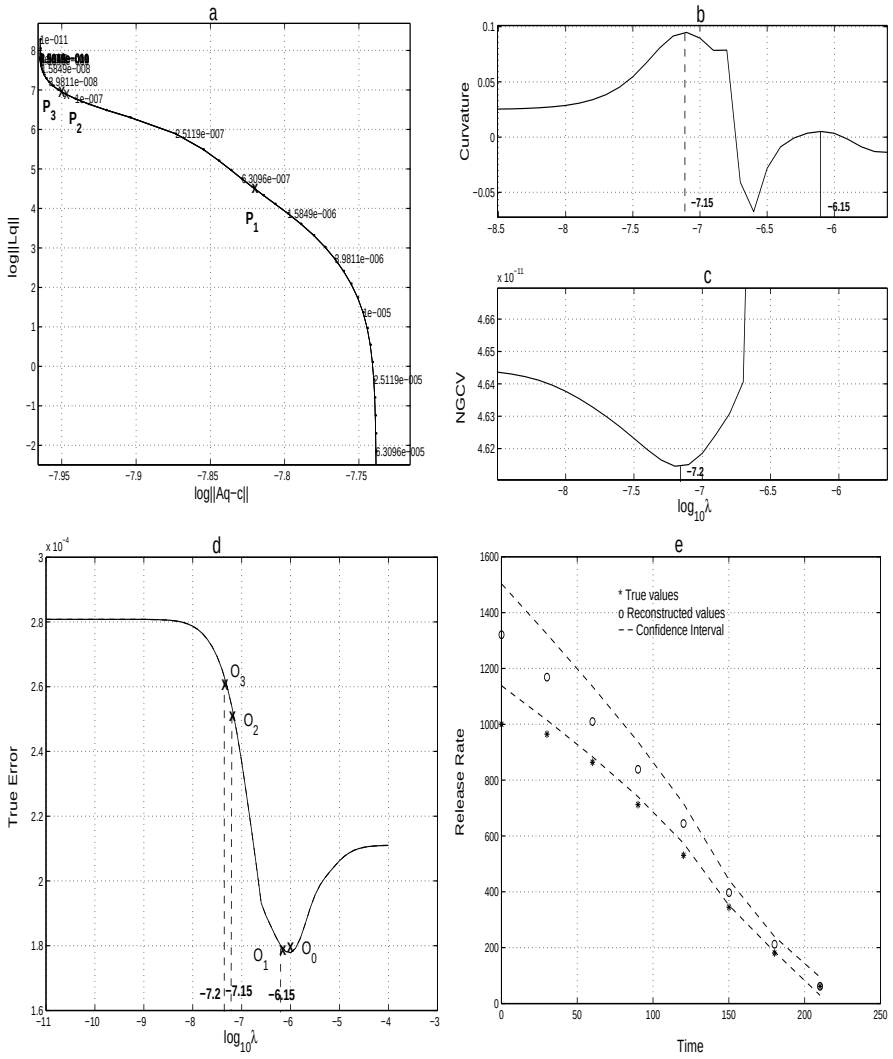

Figure 46: Example 2- data 3: (a) non-linear L-curve, (b) curvature *vs* regularisation parameter, (c) NGCV *vs* regularisation parameter, (d) true error *vs* regularisation parameter, (e) release rates *vs* time

48c–50c depict the error in the reconstructed location $\mathbf{p}$ as a function of λ. Figures 48d–50d depict the true error in the solution against different regularisation parameters. Figures 48e–50e depict the true linear parameter (release rates) along with its reconstructed value and confidence interval.

For the first set of data, P_1 is the only corner on the L-curve (Figure 48a), and point O_1 (Figure 48b) is its corresponding true error. The error at point O_1 is not zero, even though the data are perfect. This shows the effect of regularisation in the reconstructed solution. For the second set of data, P_1, P_2 and P_3 are the candidates for the optimal point on the L-curve (Figure 49a), and points O_1, O_2 and O_3 (Figure 49d) are their corresponding true errors. Point O_1 is closer to the true minimum than the other two points and therefore O_1 is our choice for the optimal point. For the third set of data, P_1, P_2, P_3 and P_4 are the four candidates for the optimal point on the L-curve (Figure 50a), and points O_1–O_4 (Figure 50d) are their corresponding true errors. Point

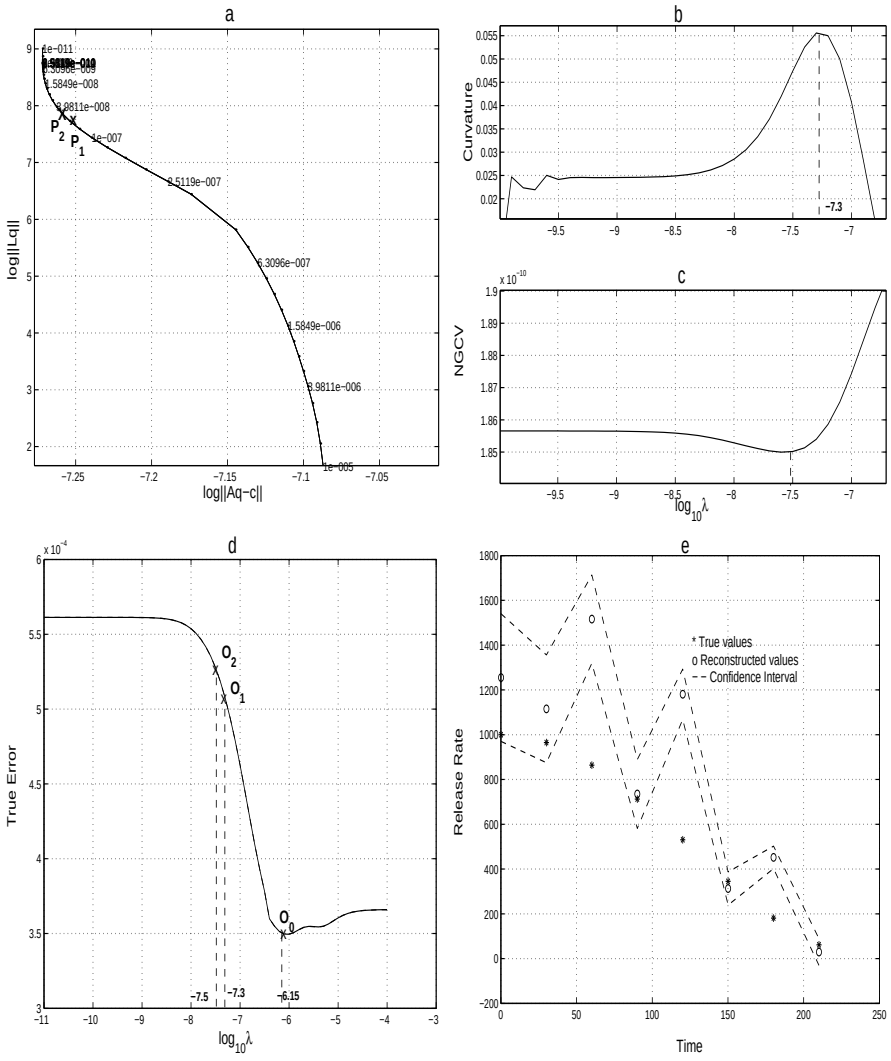

Figure 47: Example 2- data 4: (a) non-linear L-curve, (b) curvature *vs* regularisation parameter, (c) NGCV *vs* regularisation parameter, (d) true error *vs* regularisation parameter, (e) release rates *vs* time

O_1 is closer to the true minimum (O_0) and therefore the regularisation parameter that corresponds to the point P_1 is taken as the optimal value.

Important observations from these solutions are similar to the previous example, but the following differences can be observed between Examples 2 and 3:

(i) when the data are perfect, error in the reconstructed solution decreases with the increasing number of source points (decreasing the discretisation size for the source function), because the total error also contains a numerical error due to the discretisation of the integral equation (2.37). By decreasing the size of the partition of the source function the numerical error due to discretisation can be minimised;

(ii) when the data are corrupted by noise, the error in the reconstructed solution increases with the increasing discretisation parameter, because the condition number of a system matrix

Table 11: Case 3: Different number of source, data points

		Noise in the data		
		0%	1%	5%
p	True value	Estimated value ± Confidence interval		
X_0	200.00	200.75 ± 0.21	202.29 ± 1.80	200.2 ± 8.0
Y_0	30.00	30.06 ± 0.02	31.08 ± 1.38	35.2 ± 5.89
H	10.00	9.99 ± 0.001	10.10 ± 0.14	10.68 ± 0.51

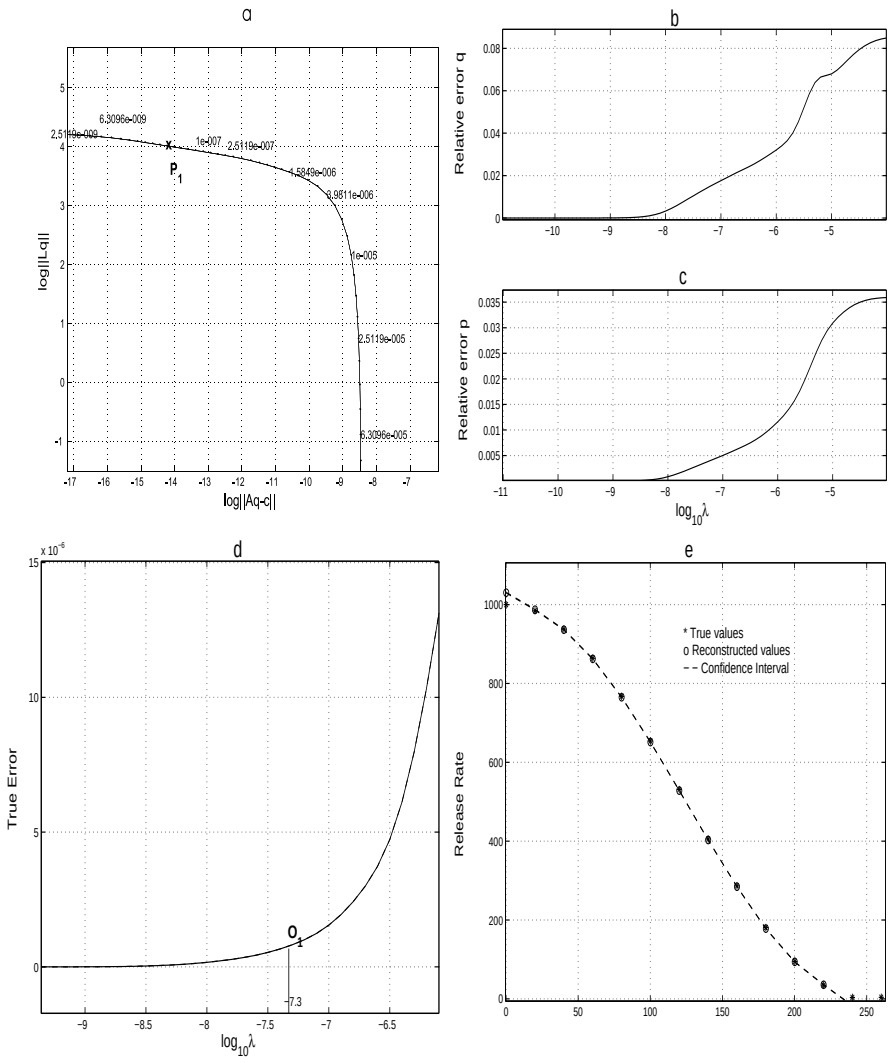

Figure 48: Example 3- data 1: (a) non-linear L-curve, (b) relative error in **q** *vs* regularisation parameter, (c) relative error in **p** *vs* regularisation parameter, (d)true error *vs* regularisation parameter, (e) release rates *vs* time

increases with the decrease of the partition size of the source function.

Further, Groetsh (4) shown that increasing the discretisation parameter (i.e. decreasing the size

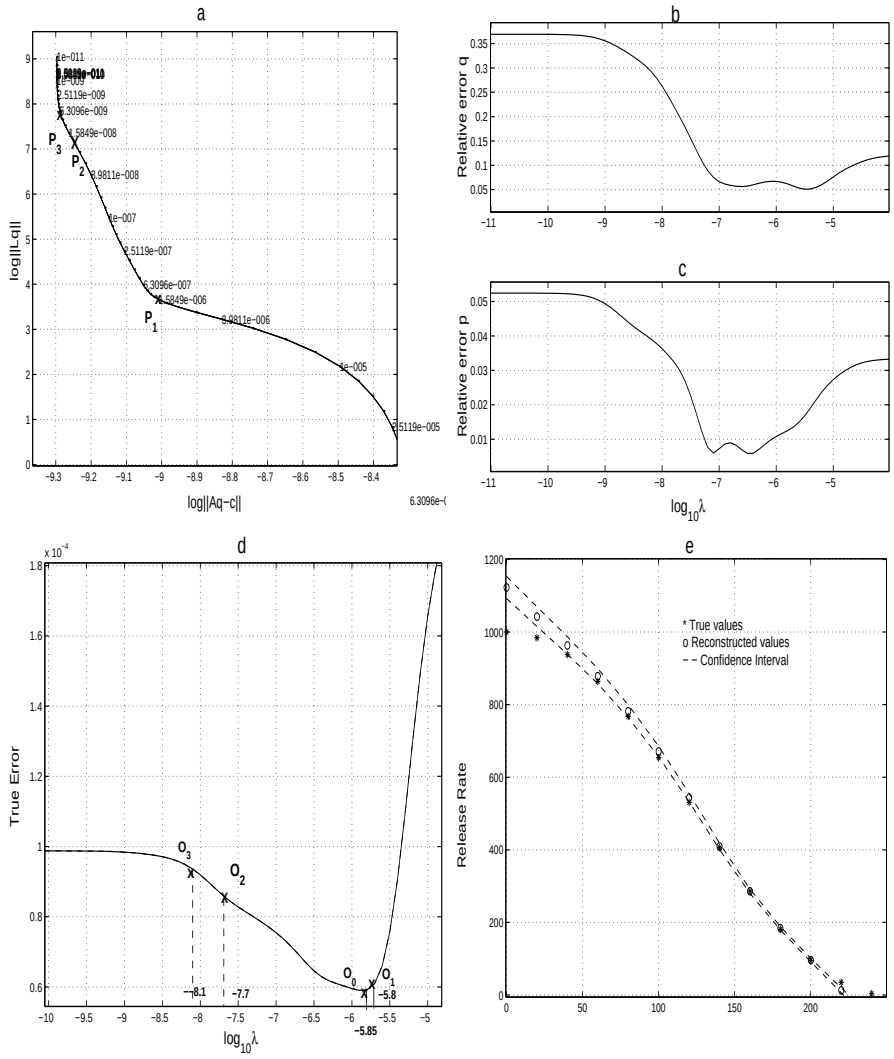

Figure 49: Example 3- data 2: (a) non-linear L-curve, (b) relative error in **q** *vs* regularisation parameter, (c) relative error in **p** *vs* regularisation parameter, (d) true error *vs* regularisation parameter, (e) release rates *vs* time

of the partition) creates a large condition number, and the upper bound on the relative solution error increases dramatically. The condition of a system matrix is a measure of ill conditioning, and we can therefore say that the accuracy of the solution depends on the degree of ill conditioning.

Example 4: Two different source functions

In this example we consider two data sets created by using two different source functions shown by stars in the Figures 51c and 52c respectively. The results of the inverse model estimation are summarised in Table 12, Figures 51 and 52. Listed in the table are the true non-linear parameter (location) values along with the reconstructed values and confidence interval estimates. The L-curve, which has a lowest function value, is shown in Figures 51a and 52a for each set of data. Figures 51b and 52b depict the true error in the solution against different regularisation parameters.

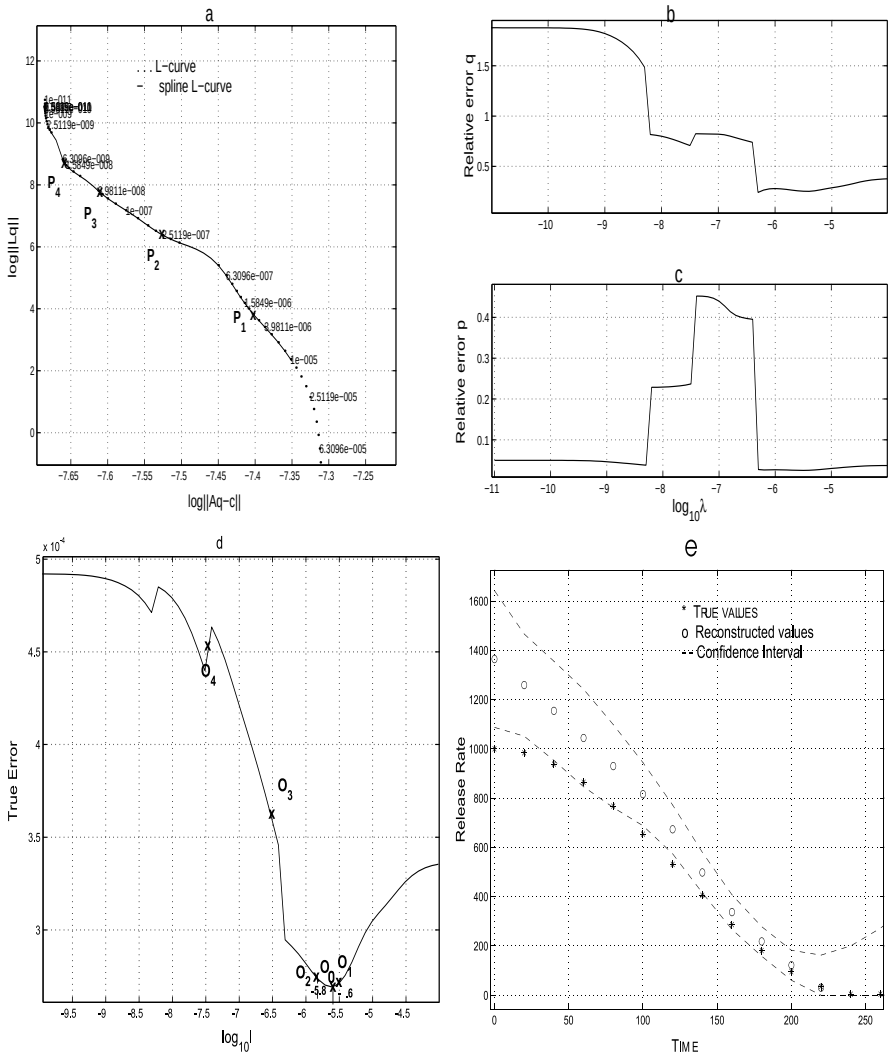

Figure 50: Example 3- data 3: (a) non-linear L-curve, (b) relative error in **q** *vs* regularisation parameter, (c) relative error in **p** *vs* regularisation parameter, (d) true error *vs* regularisation parameter, (e) release rates *vs* time

Figures 51c and 52c depict the true linear parameter (release rates) along with its reconstructed value and confidence interval. Figures 51d and 52d depict the true concentration history at the location P along with its reconstructed history.

For the first set of data, P_1, P_2 and P_3 are the three candidates for the optimal point on the L-curve (Figure 51a) and points O_1, O_2 and O_3 (Figure 51b) are their corresponding true errors. The error at the point P_1 is at the true minimum ($O_0 = O_1$) where both error due to regularisation and error due to noise are equal. Therefore P_1 is more suitable for an optimal point than other points. For the second set of data, P_1, P_2 are the candidates for the optimal point (Figure 52a) and points O_1, and O_2 (Figure 52b) are their corresponding true errors respectively. Point O_1 is closer to the true minimum and therefore the regularisation parameter that corresponds to point P_1 is more suitable for the problem than other points. The important observation from this example is that the errors in the reconstructed solutions are not equal even though the data are corrupted by

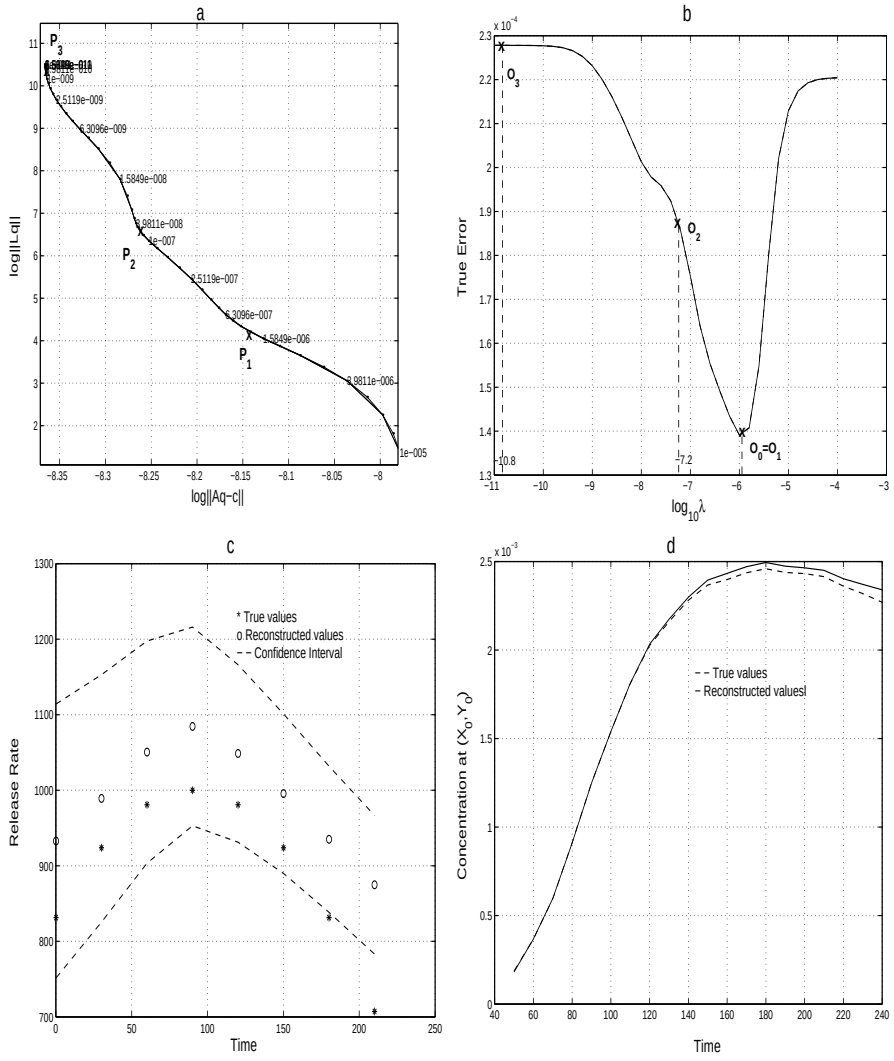

Figure 51: Example 4- data 1: (a) Non-linear L-curve, (b) true error *vs* Regularisation parameter, (c) release rates *vs* time, (d) concentration history at the point P=$(X_0, Y_0, 0)$

the same size of the same random noise.

Example 5: Source at different locations

In this example we first simulate three sets of perfect data using the same source at three different locations. Then we corrupt each set of data by adding 2%, 4% and 8% of normally distributed relative noise. The results of the source location estimation and the relative error in the release rate estimation using these corrupted data are summarised in Table 13. The important observations from Table 13 are

(i) the confidence interval of the location estimates increases with increasing source distance for the same amount of noise,

(ii) the percentage of error in the release rates increases with increasing source distance.

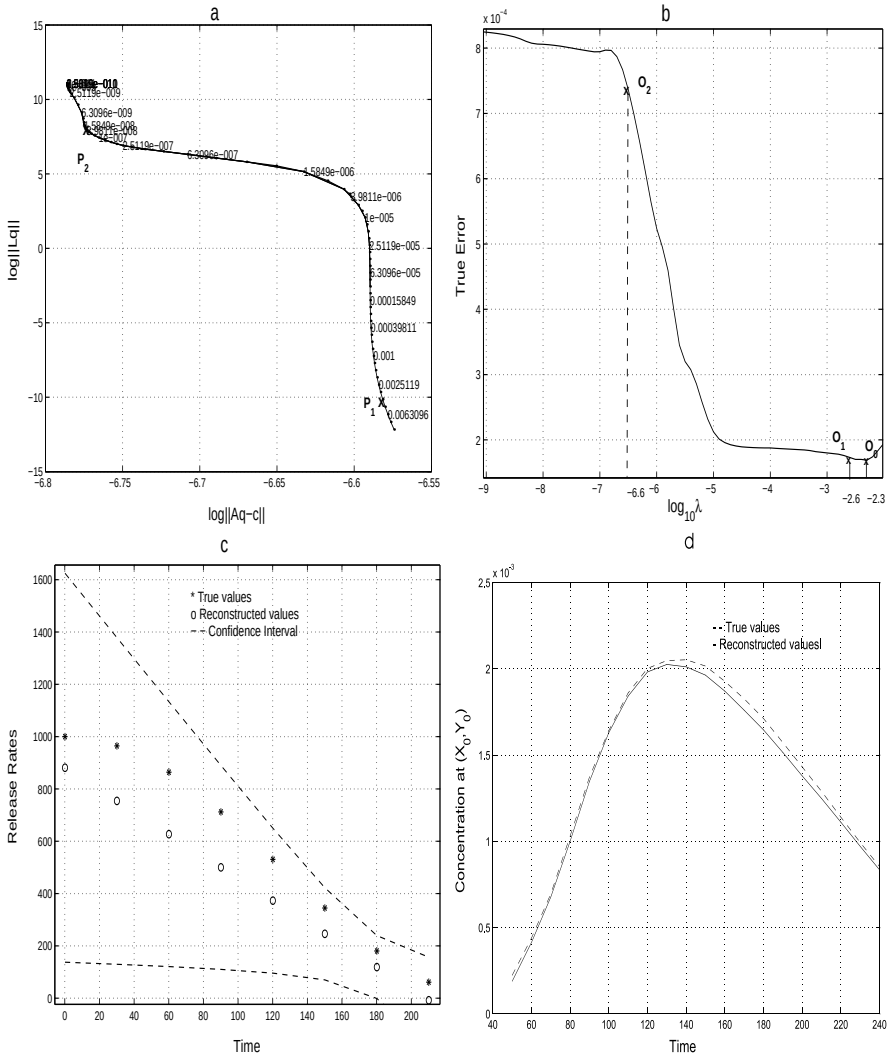

Figure 52: Example 4- data 2: (a) Non-linear L-curve, (b) true error *vs* regularisation parameter, (c) release rates *vs* time, (d) concentration history at the point P

In Chapter 5, we learned that the condition number of the coefficient matrix increases with the increasing distance between source and observation sites. But the condition number is proportional to the ill-conditioning of the coefficient matrix. Therefore the reason for the above two observation is due to ill-conditioning of the problem i.e. ill-conditioning of the problem increases with increasing distance between the source and the observation sites.

5.2 Method-3

We consider two examples to demonstrate the developed method for finding the release rate $q(t)$ and the location (X_0, Y_0, H). The purposes of this example are:

(i) to demonstrate the simultaneous estimation of parameters X_0, Y_0, H and the source release function $q(t)$;

Table 12: Case 4: Comparison of two different source functions when the measured data is corrupted with 25% random noise

	True value	Estimated value ± Confidence interval	
		data 1	data 2
X_0	150.00	151.30 ± 7.74	161.14 ± 14.80
Y_0	25.00	26.8 ± 4.10	19.0 ± 22.6
H	12.00	12.15 ± 0.35	11.50 ± 2.24

(ii) to compare the solutions obtained using methods 2 & 3

Example 6

In this example we consider a set of data that is corrupted by 10% of random noise. The results of the source-term estimation are summarised in Table 14 and Figure 53. Listed in Table 14 are the true non-linear parameter (location) values along with the reconstructed values and their confidence interval estimates. The graph of the regularisation parameter *vs* the number of calculations is shown in Figure 53a. This figure clearly shows that after a few calculations the regularisation parameter converges to 2.34×10^{-6}. Figures 53b and 53c depict the relative error in $\mathbf{q}$ and $\mathbf{p}$ respectively as a function of λ. Figure 53d depicts the true linear parameters (release rates), along with their reconstructed values and confidence interval estimation. Figure 53e depicts the true and reconstructed concentration history at the location P.

Source location ($\mathbf{p}$) estimations using method 2 are also listed in Table 14. This table also contains the optimal value of λ, the relative error in the source location estimation ($\mathbf{p}$), the relative error in the release rate ($\mathbf{q}$) estimation using each method, and a value of λ where the true error function is minimum. Since we know the true error minimum and it is therefore possible to compare the accuracy of the values obtained using methods 2 and 3. The value the regularisation parameter obtained using method 3 is closer to the value of λ where it has the lowest true error, than the value obtained using method 2. Further, the size of the confidence interval is small for method 3. Therefore, we can say that method 3 performs better than method 2. But if we consider the relative error estimates of $\mathbf{p}$ and $\mathbf{q}$, it is difficult to judge the accuracy of the methods against each other.

Example 7

In this example we consider first two examples of section 6.6.1 to compare the relative error in the location $\mathbf{p}$ and the release rates $\mathbf{q}$ estimates using methods 2 and 3. A comparison of relative errors for these examples using these methods is given in Table 15.

6 Summary and Discussion

The goal of the work presented here is to develop an inverse model capable of simultaneously estimating the location and release rate of a pollutant gas from a point source. The approach is based on a non-linear least squares estimation using pollutant concentration measurements on the ground. As the problem is ill-posed, we apply Tikhonov's regularisation method to stabilise the solution. The problem is non-linear and therefore we cannot use only linear algebra to determine the solution. In the process, we developed three different algorithms, each of which is applied to many test cases. In all of our algorithms we used the fact that some of the parameters are linear and hence can be determined using simple linear algebra. For the computation of non-linear parameters we then relied exclusively on MATLAB's routine *lsqnonlin*. This process is speeded up

Table 13: Case 5: Source at different locations

Noise in data		2	4	8
p	True value	Reconstructed vale ± Confidence interval		
X_0	800	799.6 ± 0.9	798.9 ± 1.8	795.2 ± 3.9
Y_0	100	102.8 ± 1.5	104.4 ± 2.9	100.4 ± 6.5
H	12	12.1 ± 0.2	12.2 ± 0.4	13.1 ± 0.9
		Relative error estimates in **q**		
q		0.038	0.065	0.080
p	True value	Reconstructed vale ± Confidence interval		
X_0	2800	2801.6 ± 12.9	2803.2 ± 26.1	2815.4 ± 56.6
Y_0	100	103.8 ± 20.7	106.5 ± 41.5	105.9 ± 77.8
H	12	13.9 ± 1.6	15.1 ± 3.0	14.7 ± 6.6
		Relative error estimates in **q**		
q		0.062	0.096	0.107
p	True value	Reconstructed vale ± Confidence interval		
X_0	3800	3801.2 ± 17.5	3811.2 ± 35.8	3833.31 ± 51.0
Y_0	100	103.3 ± 33.5	106.2 ± 58.3	103.90 ± 105.2
H	12	14.9 ± 3.5	19.2 ± 7.1	20.1 ± 8.3
		Relative error estimates in **q**		
q		0.155	0.216	0.256

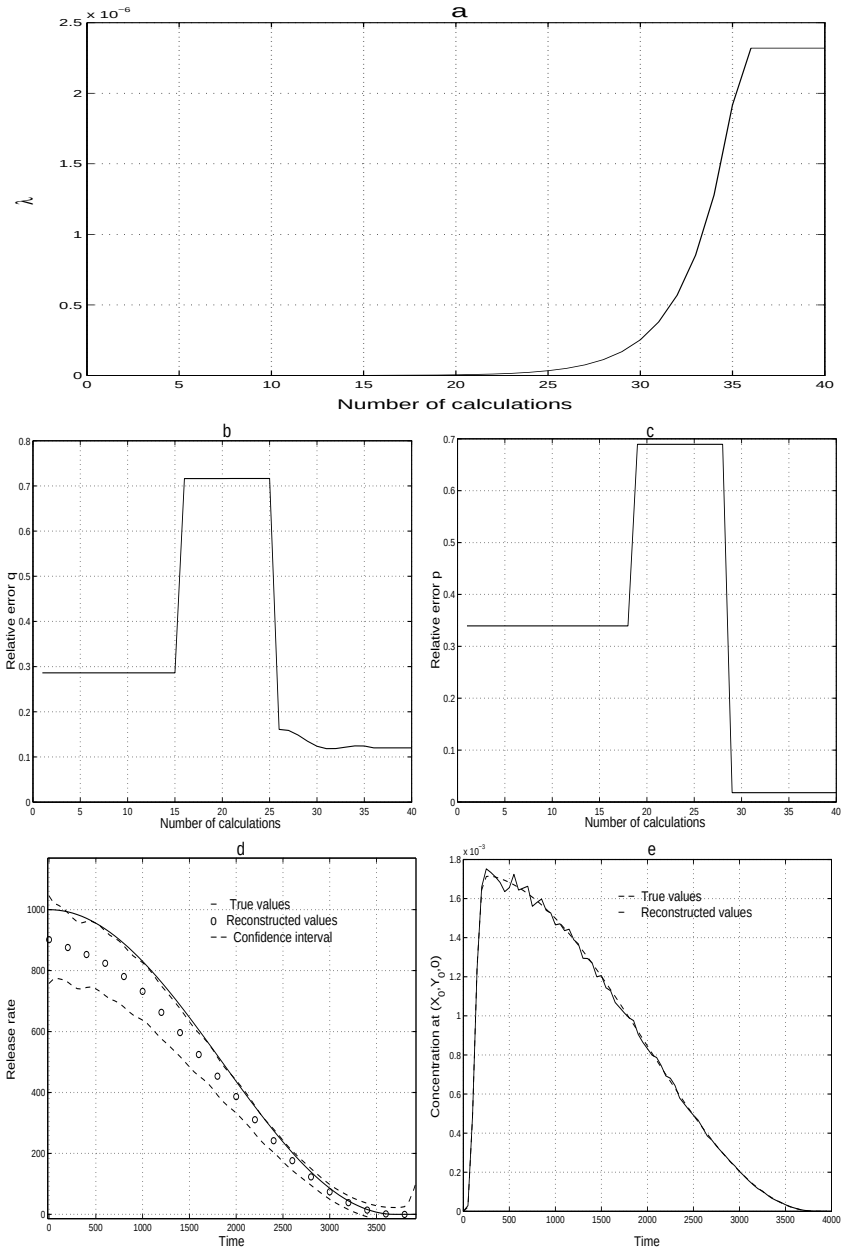

Figure 53: Method 3: (a) convergence of λ, (b) relative error in $\mathbf{q}$, (c) relative error in $\mathbf{p}$, (d) release rates *vs* time (e) concentration history at the point P=$(X_0, Y_0, 0)$

enormously because, after the elimination of linear parameters, only three non-linear parameters remain.

A series of examples given in the last section describes how the model is able to determine the location and release rate of a pollution source, and how factors such as noise in the data, regularisation and the size of discretisation affect the accuracy of the solution. The results from these examples suggest that the inverse model is capable of estimating the location and the release rate of a pollution source to a reasonable degree of accuracy. Four factors affect the accuracy of

Table 14: Example 6: Comparison of estimates using Methods 2 and 3

		Method 2	Method 3
p	True value	Estimated values ± Confidence interval	
X_0	300.0	304.0 ± 14.2	305.0 ± 12.6
Y_0	50.0	47.8 ± 10.1	47.9 ± 9.7
H	12.0	11.4 ± 0.7	11.4 ± 0.7
		Regularisation parameter estimates	
λ	1.0×10^{-5}	1.58×10^{-6}	2.34×10^{-6}
		Relative error estimates	
p		0.016	0.018
q		0.122	0.120

Table 15: Example 7: Comparison of relative error estimates Methods 2 & 3

Example No	Data set no	Parameter	Method 2	Method 3
Example 1	Data 1	**p**	0.088	0.120
		q	0.340	0.288
	Data 2	**p**	0.035	0.07
		q	0.51	0.40
Example 2	Data 1	**p**	0.012	0.000
		q	0.030	0.002
	Data 2	**p**	0.015	0.032
		q	0.075	0.112
	Data 3	**p**	0.038	0.034
		q	0.275	0.335
	Data 4	**p**	0.088	0.085
		q	0.526	0.340

the solution:

(i) size and randomness of noise in the data,

(ii) size of discretization of the source function,

(iii) regularisation, and

(iv) distance between source and observation sites.

From our observations it can be noticed that the major factor induces error in the reconstructed solution is the noise in the data. Therefore we can conclude that the total error in the solution mostly depends on inaccuracies in the data.

We employ basically two methods (method 2 and method 3) to find the optimal value of the regularisation parameter. In method 2 we solved the problem for a sequence of λ values and then we employed three different methods described in section 6.3 to picked the optimal point on the L-curve. In method 3 we also solved the problem for a sequence of λ values but here we start

from smaller λ and then decrease its value until its steady state. Both methods perform well, and one particular approach does not always predict a better result than the other method. In our experience, therefore both methods are equally useful. If we consider only the amount of computation time, then method 3 is a better choice than method 2.

References

[1] L.L. Edwards, R.P. Fries, L.G. Peters & P.H. Gudiksen, The use of non-linear regression analysis for integrating pollutant concentration measurements with atmospheric dispersion modelling for source term estimation. *Nuclear Technology*, (101), 168–181, 1993.

[2] C. G. Farquharson, and D. W. Oldenburg, A comparison of L-curve and GCV techniques for estimating the regularisation parameter in nonlinear inverse problems, *Submitted to Geophysical Journal International*, 2002.

[3] C. G. Farquharson, and D. W. Oldenburg, Automatic estimation of the trade-off parameter in nonlinear inverse problems using the GCV and L-curve criteria, *SEG 70th Annual Meeting*, Calgary, Alberta, 6 - 11 August 2000.

[4] C.W. Groetsch, *Inverse problems in the Mathematical Sciences.* Vieweg, Bruanschweig, Wiesbadden, 1993.

[5] M. E. Gulliksson, and P. A. Wedin P, Algorithms for using nonlinear L-curve *Submitted to SIAM Journal of Optimisation*, 1998.

[6] m. E. Gulliksson, and P. A. Wedin, Analyzing the nonlinear L-curve, *Submitted to SIAM Journal of Optimisation*, 1998.

[11] M. E. Gulliksson and P. A. Wedin, Algorithms for using the non-linear L-curve. *Submitted to SIAM J. Optim* , 1998.

[8] C.P. Hansen, *Rank-deficient and discrete ill-posed problems.* SIAM, Philadelphia, PA, 1997.

[9] C.P. Hansen, *Regularisation tools: A MATLAB package for analysis and solution of discrete ill-posed problems* Danish Computing Center for Research and Education, 1993.

[10] E. Haber E, and D. W. Oldenburg, A GCV based method for non-linear ill-posed problems, *Computational Geosciences*, 4, 41–63, 2000.

[11] P. Kathirgamanathan, R. McKibbin and R.I. McLachlan, Source term estimation of pollution from an instantaneous point source. *MODSIM*, (6)2:1013–1018, 2001.

[12] P. Kathirgamanathan, R. McKibbin and R.I. McLachlan, Source release rate estimation of atmospheric pollution from non-steady point source at known location. *Submitted to the Journal of Environmental Modelling and Assessment*, 2002.

[13] J.F. Kibler & J.T. Suttles, Air pollution model parameter estimation using simulated LIDAR data. *AIAA Journal*, (15)10, 1381–1384, 1977.

[14] R.H. Myers, *Classical and modern regression with applications.* Duxbury Press, Boston: PWS-KENT, 1990.

[15] P.S. Mahar, Identification of pollution sources in transient groundwater systems. *Water Resources Management*, (14), 209–227, 2000.

[16] A.D Woodbury & T.J. Ulrych, Minimum relative entropy inversion: Theory and application to recovering the release history of a groundwater contaminant. *Water Resources Research*, (32), 2671–2681, 1996.

[17] T.H. Skaggs and J.K. Kabala, Recovering the release history of a ground water contaminant using a non-linear least squares method. *Water Resources Research*, (30)1, 71–79, 1994.

[18] T.H. Skaggs and J.K. Kabala, Recovering the history of a ground water contaminant plume: method of quasi-reversibility. *Water Resources Research*, (31)11, 2669–2673, 1995.

[19] T.H. Skaggs and J.K. Kabala, Recovering the release history of a ground water contaminant. *Hydrological Process*, (14)1, 1003–1016, 2000.

[20] D. M. Trujillo, and H. R. Busby H, Practical inverse analysis in engineering, *CRC Press*, Boca Raton, New York, 1997.

[21] B.J. Wanger, Simultaneous parameter estimation and contaminant source characterization for coupled groundwater flow and contaminant transport modelling. *Journal of Hydrology*, (135), 275–303, 1992.